보건학석사 학위논문

Performance Evaluation of Analytical Method for Nanoparticles using a Single Particle Inductively Coupled Plasma and Application to Nanoparticle-containing Consumer Products

SP-ICP-MS를 이용한

나노물질 분석 방법 성능평가 및 응용

2017년 8월

서울대학교 보건대학원

환경보건학과 산업보건전공

유 단 비

ABSTRACT

Performance Evaluation of Analytical Method for Nanoparticles using a Single Particle Inductively Coupled Plasma and Application to Nanoparticle-containing Consumer Products

Danbi Yoo
Department of Environmental Health Sciences
Graduate School of Public Health
Seoul National University, Korea

Advisor Chungsik Yoon, Ph.D, CIH

Objective Single particle inductively coupled plasma (SP-ICP-MS) is a promising technique to detect nanosized inorganic particles at very low concentrations. The purpose of this study was to validate analytical procedures for detecting nanoparticles (NPs) in solution using SP-ICP-MS and to apply these procedures for the analysis of Ag and TiO_2 NPs in a consumer spray product.

Methods The performance evaluation experiment tested the accuracy, precision, and stability of analytical procedures using three sizes of Ag and TiO_2 reagents.

Accuracy was evaluated with regards to both size accuracy and recovery of particle concentration. Relative standard deviation (RSD) and pooled RSD were used to verify precision. Stability during storage was evaluated at zero, one, four, seven and fourteen days after storage. Before characterizing the nanoparticles in consumer products, six different kinds of pretreatment methods were compared to select appropriate pretreatment methods (water, ethanol, and ethanol evaporation) on the basis of accuracy and precision. A total of ten consumer products (three of them were labelled as containing Ag NPs, three of them were labelled as containing TiO_2 NPs, and four of them were not labelled as containing NPs) were analyzed with SP-ICP-MS using the optimal pretreatment method, transmission electron microscopy equipped with an energy-dispersive X-ray spectrometer (TEM-EDS), and field emission scanning electron microscope with an energy-dispersive X-ray spectrometer (FE-SEM-EDS).

Results Accuracy and precision were in the acceptable range according to the NIOSH guidelines for air sampling and analytical method development and evaluation. Size accuracy was higher than 95% (96–115%), with the exception of 30 and 50 nm TiO_2 NPs (121–237%). Calibration lines of particle concentrations were linear and showed correlation coefficients of >0.99. Recovery of particle concentration was 91-109% with the exception of 30 nm TiO_2 NPs. The RSD value to evaluate precision was 0.01–6.21, with the exception that the most frequent size data of TiO_2 was 0.18–106.88. The accuracy and precision differences between Ag and TiO_2 were due to the stability and characteristics of the reagents. It is recommended that samples are analyzed as quickly as possible for accurate size

and particle concentration analysis; the time should not exceed one day. When samples contained a mixture of sizes, the recovery of bigger sized particles was over 100%, and the recovery of smaller sized particles was under 50%. The best treatment method was the Tween 80 method, wherein 0.1% of Tween 80 was added to the solution; this was not the optimal method for TiO_2 analysis with a water base. According to SP-ICP-MS analysis, all of the consumer spray products contained Ag NPs and eight of the consumer spray products contained TiO_2 NPs. The sizes of Ag NPs in the consumer spray products ranged from 27 to 81 nm, and particle concentrations ranged from 4.7×10^5 to 3.9×10^7 particles/mL. The sizes of TiO_2 NPs in the consumer spray products ranged from 35 to 65 nm, and particle concentrations ranged from 7.7×10^7 to 9.2×10^8 particles/mL. SEM and TEM analyses also yielded similar sizes and concentrations.

Conclusion SP-ICP-MS is an analytical method for analyzing metallic NPs and has a number of unidentified technical issues. Analyses of Ag NPs and larger sized TiO_2 NPs provided reliable data; however, analyses of smaller sized (<50 nm) TiO_2 NPs and mixtures of different sized NPs were unreliable. Ten of the consumer products contained nanosized Ag particles, and eight of the consumer products contained nanosized TiO_2 particles. The number of Ag NPs and TiO_2 NPs in consumer products was over a hundred thousand. The results obtained from the analyses of consumer spray products could be applied to exposure assessments of consumer products. With further method validation, the SP-ICP-MS method could characterize the particle size and particle number concentration of diverse samples.

Keywords: Single particle ICP-MS, Consumer products, Silver, Titanium dioxide, Performance evaluation, Nanoparticles, Pretreatment.

Student Number: 2015-24109

Contents

List of Tables

List of Figures

1. Introduction

Due to the growth of nanotechnology, the use of engineered nanoparticles (ENPs) is dramatically increasing in a wide range of industries (Nowack et al., 2012). The use of ENPs in consumer products can potentially result in the release of ENPs into the environment and may negatively affect human health (Stone, 2009); therefore, the detection and characterization of ENPs in consumer products is important to assess the consequences of exposure. Proper tools and methodologies are needed for measuring ENPs in consumer products to assess their risk to the environment and human health (Klaine et al., 2008; Maynald et al., 2006). Several analytical techniques have been introduced to measure particle size and distribution such as dynamic light scattering (DLS), transmission electron microscopy (TEM), centrifugal particle sedimentation (CPS), and nanoparticle tracking analysis (NTA) (Hassellöv et al., 2008; Dudkiewicz et al., 2015). One limitation of DLS is it does not provide information about particle composition. A second limitation of DLS is it does not give an accurate size distribution if a sample has a broad size distribution (Sapsford et al., 2011). TEM, while quite accurate, requires sample preparation and is expensive; additionally, TEM possesses a limited field examination (Calzolai et al., 2012). CPS is unreliable in measuring particle size without exact particle density when aggregated particles are dispersed in a sample; thus it can influence the data stability. NTA is compatible with a broader size distribution than the other methods; however, NTA does not differentiate between mixed metal particles (Dudkiewicz et al., 2015; Mahl et al.,

2011). All of these techniques are not appropriate for environmental matrices that have lower concentrations of ENPs than the detection limits of many size detecting techniques (Boxall et al., 2007; Pace et al., 2012; Gottschalk et al., 2009). On the other hand, single particle inductively coupled plasma (SP-ICP-MS) has a higher sensitivity than other techniques for detecting metal nanoparticles (NPs) in environmental matrices; in addition, SP-ICP-MS can selectively detect a target NP even if several kinds of metal NPs are mixed. SP-ICP-MS has the advantages of uncomplicated procedures for sample preparation and a short run time for analysis. In addition, it can also provide information on particle size, number concentration, and elemental composition of metallic nanomaterials.

Recently, SP-ICP-MS has been applied to analyzing the heavy metallic NP content in waste water, cosmetics, and food (Dan et al., 2015; Donovan et al., Miranto et al., 2012; 2016; Peters et al., 2014; Reed et al., 2014; Verleysen et al., 2015; Witzler et al., 2016;). However, the appropriate pretreatment method for use with SP-ICP-MS has not been established with certainty; therefore, in this study, the pretreatment method that was recommended from the instrument manufacturer was adjusted according to the sample matrix. SP-ICP-MS still needs to be tested with many other sample matrices and consumer products.

Both silver (Ag), the most advertised nanomaterial, and titanium dioxide (TiO2), the most produced nanomaterial worldwide, are the main additives in consumer products due to their antibacterial functions (Nowack et al., 2011; Vance et al., 2015). Ag NPs can cause negative effects, including loss of mitochondrial

activity and DNA damage (Choi et al., 2008; Foldbjerf et al., 2009). TiO2 NPs have been reported to cause oxidative stress, carcinogenesis, and immune disruption through skin and pulmonary exposure (Shakeel et al., 2016; Shi et al., 2013; Fabian et al., 2008). In particular, spray products greatly affect the respiratory system due to their high emission potential (Losert et al., 2014); therefore, it is important to assess the risk of these consumer products by investigating the characteristics of Ag and TiO2 NPs. To date, NPs in consumer products have been analyzed using inductively coupled plasma-optical emission spectroscopy (Benn et al., 2010; Lorenz et al., 2012), inductively coupled plasma-mass spectroscopy (Quadros et al., 2011; Quadros et al., 2013), and asymmetric flow field flow fractionation-inductively coupled plasma mass spectrometry (Cascio et al., 2014). Currently, there are no mandatory regulations that require products to indicate on labels whether they contain NPs. The enactment of labeling laws requiring products to indicate if they contain NPs should be considered because of the dangers of NPs. The objectives of this study were twofold: (i) evaluate analytical procedures for detecting nanoparticles in solution using SP-ICP-MS; and (ii) apply the evaluated method to analyzing Ag and TiO2 NPs in consumer spray products.

2. Materials and Methods

2.1. Study outline

The overall outline of this study is shown in Figure 1. This study consisted of three parts. In the first part, a performance evaluation of SP-ICP-MS was performed. In the second part, the proper pretreatment methods were determined for each base and target analyte. Lastly, consumer products were analyzed with SP-ICP-MS and electron microscopy.

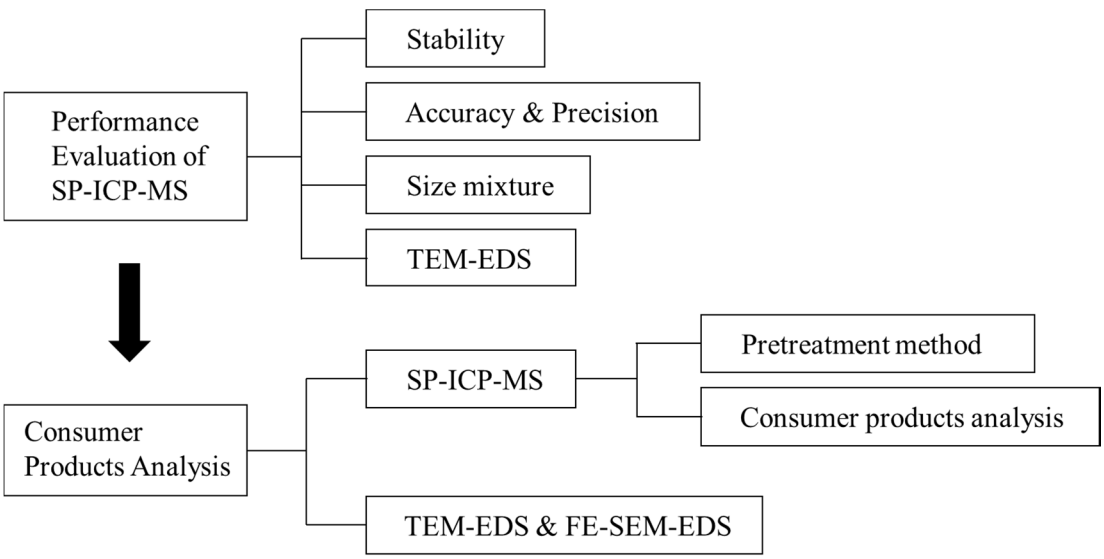

Figure 1. The outline of this study.

2.1.1. Subjects

Three types of NPs were used in this study: a gold (Au) NP solution, a Ag NP solution, and a TiO_2 NP nanopowder. Au nanoparticles in aqueous suspension were acquired in sizes of 30 nm (N8142300, 30 nm Spherical gold nanoparticle in DI water, PerkinElmer, USA), 50 nm (N8142302, 50 nm Spherical gold nanoparticle in DI water, PerkinElmer, USA), and 70 nm (N8142304, 70 nm Spherical gold nanoparticle in DI water, PerkinElmer, USA) to calibrate the size and measure the transport efficiency of SP-ICP-MS. Solutions of Ag NPs were purchased as follows: 30 nm Ag NPs (730793, Silver dispersion, Sigma-Aldrich, USA); 60 nm Ag NPs (730815, Silver dispersion, Sigma-Aldrich, USA); and 100 nm Ag NPs containing sodium citrate as a stabilizer (730777, Silver dispersion, Sigma-Aldrich, USA). TiO_2 nanopowders were purchased as follows: 30 nm TiO_2 powder (US3520, Titanium Oxide Nanopowder (rutile), US Research Nanomaterials, USA); 50 nmTiO_2 powder (US3530, Titanium Oxide Nanopowder (rutile), US Research Nanomaterials, USA); and 100 nm powder (US3535, Titanium Oxide Nanopowder (rutile), US Research Nanomaterials, USA). These reagents were used to evaluate the precision, accuracy, and sample stability of the SP-ICP-MS analytical method.

Dissolved Au (N9303759, Gold pure single-element standard, PerkinElmer, USA), Ag (N9300151, Silver pure single-element standard, PerkinElmer, USA), and Ti (N9300162, Titanium pure single-element standard, PerkinElmer, USA) standards were used for dissolved element calibration. Solutions were diluted with deionized water (DW) from a Milli-Q water purification system unit (Millipore, Bedford, MA, USA).

2.1.2. Instrument condition

To measure particle size, particle number concentration, and metallic ion concentration, a NexION 350D ICP-MS (PerkinElmer, Waltham, MA, USA) was used. Data were recorded using PerkinElmer Syngistix software with NanoApplication and exported as a Microsoft Excel file. The detailed instrumental conditions are shown in Table 1. The TiO_2 mass was converted according to equation 1 (Dan et al., 2015).

$$m = \rho \times V = \rho \frac{\pi}{6} D^3 \cdots\cdots\cdots\cdots\cdots\cdots\cdots\cdots \text{equation (1)}$$

where m=mass of a spherical TiO_2 particle, ρ=density of TiO_2, V=volume of a spherical TiO_2 particle with a diameter of d, and d=diameter of a spherical TiO_2 particle. The density of rutile TiO_2 was 4.23 g/cm3 used because of near spherical shape of rutile TiO_2.

To confirm the morphology of nanoparticles, transmission electron microscopy (JEM-1010, JEOL, Japan) was used equipped with an energy dispersive spectroscopy (EDS, Model AZtecOneXT, Oxford Instruments Inc., UK) and field emission scanning electron microscope (MERLIN compact, ZEISS, Germany) in conjunction with EDS analysis.

Table 1. Instrument and method parameter for SP-ICP-MS analysis

Instrument parameter	Operation setting	
Nebulizer	Concentric Glass	
Spray chamber	Cyclonic	
Sampler cone	Nickel 1.0 mm	
Skimmer cone	Nickel 0.9 mm	
RF power (W)	1600	
Nebulizer gas flow (L/min)[1)]	0.96	
Auxiliary gas flow (L/min)	1.2	
Plasma gas flow (L/min)	18	
Sample flow rate (mL/min)[1)]	0.31~0.35	
RPq[2)]	0.25	
Dwell time (ms)	0.1	
Sample time (s)	100	
Transport efficiency (%)[1)]	7.5-8.5	
Method parameters	Ag	Ti
Isotope (amu)	107	47
Density (g/cm^3)	10.49	4.23
Mass fraction (%)	100	60
Ionization efficiency (%)	100	100

[1)]parameter optimized daily
[2)]Quadrupole dynamic band-pass tuning parameter

2.2. Performance evaluation of SP-ICP-MS

2.2.1. Sample preparation

To measure the transport efficiency and calibrate the size of the SP-ICP-MS, 30, 50, and 70 nm Au NPs were diluted with DW to a particle concentration of approximately 10^5 particles/mL. The calibrations for dissolved Au, Ag, and TiO_2 were performed with three concentrations (2, 5, and 10 ppb) of each analyte. Three replicates of each concentration of each sample were made; thus, each sample concentration was measured three times. For readability, the particle number concentration was converted to a particle mass concentration. All data gathered from the performance evaluation were evaluated according to the NIOSH guidelines for air sampling and analytical method development and evaluation (Eugene et al., 1995)

Stability

On the basis of recovery and RSD values, one particle concentration was selected for each NP size (Ag: 0.004 ppb of 20 nm, 0.077 ppb of 60 nm, and 0.313 ppb of 100 nm and TiO_2: 0.250 ppb of 30 nm, 1.667 ppb of 50 nm, and 20.000 ppb of 100 nm).

Accuracy & Precision

Four spike particle mass concentrations (Table 2) in each size of Ag and TiO_2 NP solutions were prepared to evaluate accuracy and precision. The particular concentrations used avoided multiple particles being counted as one when particles

pass the detector (Witzler et al., 2016). One concentration in each size of Ag and TiO_2 was selected.

Size mixture

A total of three sizes were mixed to verify the recovery of particle mass concentrations for both Ag and TiO_2. To avoid overlapped particles counting as one, particle mass concentrations were prepared to have approximately 10^5 to 10^7 particles/mL. The Ag particle mass concentrations used were 0.1900 ppb, 0.2847 ppb, and 0.3795 ppb. The TiO_2 particle mass concentrations used were 3.9333 ppb, 7.8667, and 9.8333 ppb. The specific particle mass concentrations are listed in the supplementary information (Appendix 1).

TEM-EDS and FE-SEM-EDS

All nanoparticle suspensions were analyzed to ascertain size and shape. Samples with 0.1% triton X-100 (X100, Triton X-100, Sigma-Aldrich, USA) were sonicated for five minutes; then, 10 μL of the sample was placed on a carbon-coated 200 mesh copper grid (EMS200-Cu, Electron Microscopy Sciences, PA, USA) for TEM-EDS analysis and a second 10 μL aliquot of the sample was placed on a polycarbonate membrane filter (225-1609, polycarbonate filters, SKC, USA) for FE-SEM-EDS analysis. Samples were dried at room temperature (temperature: 20 ℃ ± 5 ℃, humidity: 35% ± 5%).

Table 2. Four levels of particle mass concentration for performance evaluation experiment

Substance	Size (nm)	Level	Particle mass concentration (μg/L)
Ag	20	1	0.002
		2	0.003
		3	0.004
		4	0.007
	60	1	0.048
		2	0.077
		3	0.096
		4	0.192
	100	1	0.188
		2	0.313
		3	0.376
		4	0.752
TiO_2	30	1	0.020
		2	0.100
		3	0.200
		4	0.250
	50	1	0.333
		2	1.000
		3	1.667
		4	2.500
	100	1	10.000
		2	16.667
		3	20.000
		4	25.000

2.2.2. Sample analysis

Stability

Analysis of sample stability during storage was performed at zero, one, four, seven and fourteen days after storage. Samples were stored for fourteen days under room temperature conditions (temperature: 20℃ ± 5℃, humidity: 35% ± 5%). Stability was evaluated at the specified time intervals if the size accuracy and recovery of particle mass concentration were in the range of ± 10%.

Accuracy & Precision

Using level 1 to 4 particle mass concentrations in each size, Ag and TiO_2 were analyzed for accuracy and precision. Recovery based on each particle size and mass concentration was calculated as an index of accuracy according to equation 2.

$$\text{Recovery } \% = \frac{Spiked\ sample\ value - Unspiked\ sample\ value}{Amount\ spiked\ value} \times 100 \quad \cdots\text{equation (2)}$$

The pooled relative standard deviation (RSD) was calculated as an index of precision RSD and replicated according to equation 3 (Sklerov et al., 2011).

$$RSD_{pooled} = \sqrt{\frac{(n_1-1)\cdot {RSD_1}^2 + (n_2-1)\cdot {RSD_2}^2 + (n_3-1)\cdot {RSD_3}^2}{(n_1-1)+(n_2-1)+(n_3-1)}} \quad \cdots\cdots\cdots\text{equation (3)}$$

Size mixture

Particle mass concentration was calculated in accordance with particle size distribution for each size according to equation 4.

$$\text{Particle mass concentration} = \mathrm{N}\frac{\pi}{6}D^3\rho \quad \cdots\cdots\cdots\cdots\cdots\text{equation (4)}$$

where N=particle number concentration, D=particle diameter, ρ=density of particle. The density of TiO_2 was 4.23 g/cm^3 and the density of Ag was 10.49 g/cm^3.

2.3. Selection of pretreatment

2.3.1. Sample preparation

The same reagents used for the performance evaluation of the analytical method were used for the selection of the pretreatment method. To compare pretreatment methods for consumer product analysis, Triton X-100 (Triton X-100 laboratory grade, Sigma-Aldrich, USA) and Tween 80 (P1379, Tween 80 – viscous liquid, Sigma-Aldrich, USA) were used to disperse the nanoparticles in each sample. Ethyl alcohol (34963, 99.9% purity, Sigma-Aldrich, USA) was used to identify the proper pretreatment method for an ethanol base sample.

One spiked NP sample (0.313 ppb of 100 nm Ag and 20 ppb of 100 nm TiO_2) was selected on the basis of recovery and RSD values among all sizes and particle mass concentrations; it was used for a pretreatment method experiment.

Before analyzing the spray products using SP-ICP-MS, the pretreatment method was divided into three type of bases (water, ethanol, and ethanol evaporation) and six methods (methods A to F) to find a proper method. Each base was tested with the same six methods (Figure 2). The basic pretreatment method involved diluting 1 mL of the NP spiked sample to 10 mL using DW (Method A). Method B added sonication to method A at 40 kHz for five minutes. In method C, 0.1% Triton X-100 was added to method A. In method D, sonication for five minutes was added to method C. Method E involved adding 0.1% Tween 80 to method A. In method F, five minutes of sonication was added to method E. In the experiment using an ethanol base, 1 mL of ethanol was added to method A. In the

experiment using ethanol evaporation as the base, the ethanol was boiled at 80 ℃ for 15 minutes to evaporate the ethanol; the sample was refilled to 10 mL using DW.

2.3.2. Sample analysis

The proper pretreatment method was chosen on the basis of accuracy and precision. Recovery was calculated as an index of accuracy according to equation 2,

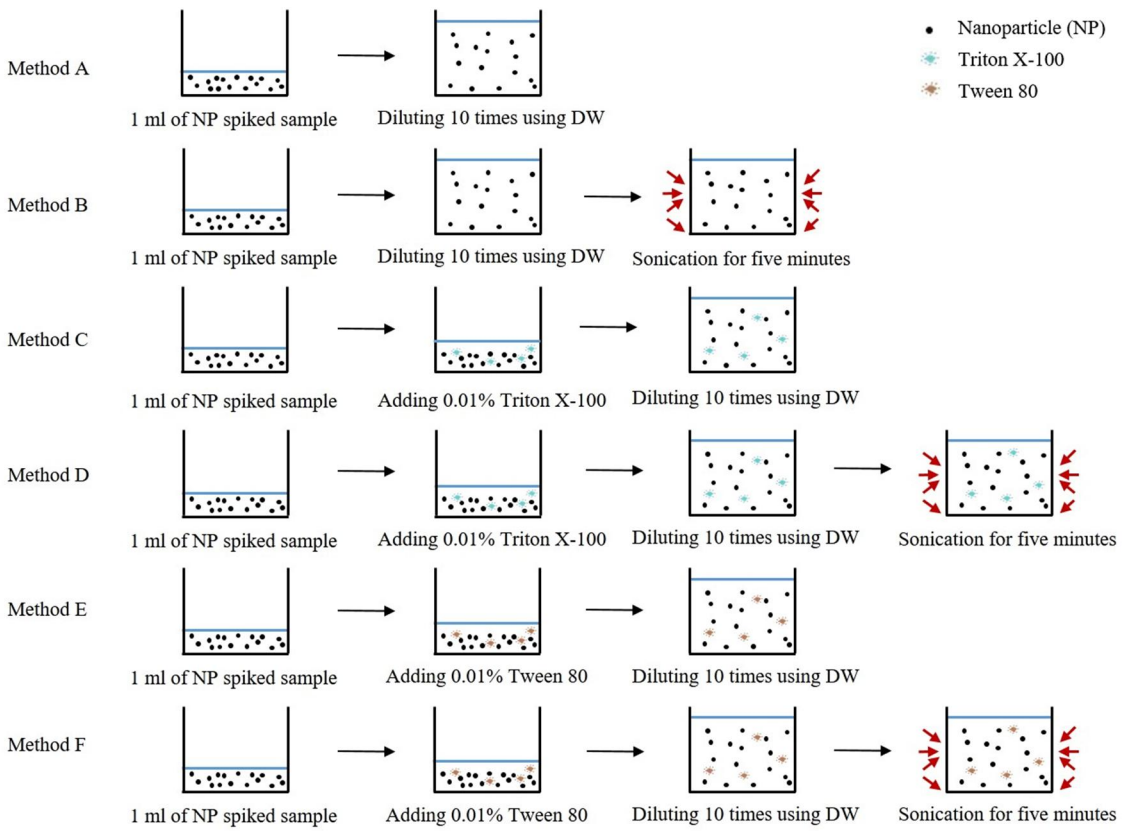

and RSD was calculated as an index of precision.

Figure 2. Schematic diagram of the six pretreatment methods. Each method was tested in each of the base types (water, ethanol, ethanol evaporation).

2.4. Consumer products analysis

2.4.1. Subjects

A total of ten consumer spray products were selected based on their internet sales indexes. Four products were labeled as "containing silver nanoparticles", and three products were labeled as "containing TiO_2 nanoparticles." Other products without labels about containing nanoparticles were chosen to compare with the nano-containing products. The information for the selected products is listed in Table 3.

Table 3. Selected consumer spray products

Product	Intended use	Mixed Solvent	Solvent content (%)	Declared NP[1)]	NP content (%)	Spray type	Other declared ingredient
A	Air deodorizer	Water	>90	Ag	NI[2)]	Trigger	Natural fragrance
B	Air deodorizer	Water	>90	Ag	NI	Trigger	Inorganic antimicrobial
C	Deodorizer for car air conditioner	Ethanol	40 ~ 50	Ag	NI	Propellant	Surfactant
D	Deodorizer for car air conditioner	Ethanol	50 ~ 60	Ag	1 ~ 3	Propellant	Fragrance
E	Air deodorizer	Water	97	TiO_2	3	Trigger	NI
F	Air deodorizer	Water	97	TiO_2	3	Trigger	NI
G	Deodorizer for car air conditioner	Water	97	TiO_2	3	Trigger	NI
H	Air deodorizer	Water	>90	-[3)]	-	Trigger	Surfactant
I	Deodorizer for car air conditioner	Ethanol	50 ~ 60	-	-	Propellant	Fragrance
J	Fabric conditioner	Ethanol	>50	-	-	Trigger	Anti-static agent

[1)] Nanoparticle
[2)] No information
[3)] No label about target NP

2.4.2. Sample preparation

SP-ICP-MS analysis was conducted to determine the size and concentration of Ag and TiO_2 NPs in consumer products. Based on the pretreatment method experiment, the most proper methods were selected and used in analyzing consumer products with SP-ICP-MS. Those pretreatment methods were as follows: 0.1% Tween 80 in a water base and 0.1% Tween 80 in an ethanol evaporation base for Ag NP analysis; 0.1% Triton X-100 in a water base and and 0.1% Tween 80 in an ethanol base for TiO_2 NP analysis.

To observe the morphology of nanoparticles, TEM-EDS and FE-SEM-EDS analyses were conducted. The same TEM and SEM instruments were used as those used in the method validation analysis. The samples were sonicated for five minutes and centrifuged at 4000 rpm before placing 10 μL of the sample on a carbon 200 mesh copper grid (Q225CR, holey carbon grids, Quantifoil, Germany) and 10 μL of the sample on a polycarbonate filter. The samples were dried at room temperature conditions.

2.4.3. Sample analysis

The size detection limit was calculated as the average intensity three times of the standard deviations of blank. The size distribution data was scattered, so the smooth function in MATLAB R2015a was applied to show a sleek distribution (Azimi et al., 2015).

3. Results

3.1. Performance evaluation of analytical method

3.1.1. Stability

To identify the stability of each sample, one concentration level of each particle size was analyzed on days zero, one, four, seven and fourteen under the same analytical conditions. The selected concentrations of each size were chosen on the basis of size accuracy and recovery of particle concentration as follows—Ag: 0.004 ppb of 20 nm, 0.077 ppb of 60 nm, and 0.313 ppb of 100 nm and TiO_2: 0.250 ppb of 30 nm, 1.667 ppb of 50 nm, and 20.000 ppb of 100 nm. The variations of particle size and particle concentration are shown in figure 3.

The mean sizes of all Ag and TiO_2 particles decreased over time. The range of decrease varied according to particle size and time. The mean particle diameter of TiO_2 particles decreased more than the diameter of Ag particles. After fourteen days, Ag particle sizes decreased by 6.1 - 33.6 % (20 nm: 14.5% (22.7 to 19.4 nm), 60 nm: 33.6% (57.4 to 38.1 nm), and 100 nm: 6.1% (114.8 to 107.9 nm)). TiO_2 particle sizes decreased by 15.2 - 42.8% (30 nm: 41.2% (65.3 to 37.3 nm), 50 nm: 15.2% (80.9 to 68.6 nm), and 100 nm: 42.8% (124.2 to 71.1 nm)). Particle size decreased slightly on day one, with the exception of 60 nm Ag particles. After day four, particle size decreased rapidly.

Particle concentrations of both Ag and TiO_2 decreased over time. The Ag particle concentration loss was greater than the TiO_2 particle concentration loss.

After fourteen days, the Ag particle concentration declined by 73.09 - 89.81% (20 nm: 98.92% to 23.44%, 60 nm: 100.23% to 10.43%, and 100 nm: 109.99% to 36.90%), and the TiO_2 particle concentration declined by 43.28 - 59.11% (30 nm: 93.30% to 38.02%, 50 nm: 90.11% to 46.83%, and 100 nm: 101.31% to 42.20%). Particle concentration decreased from day one, particularly for 20 nm Ag particles. After four days, the particle concentration decreased dramatically.

The decrease in size and particle concentration can be explained by the agglomeration of particles (Appendix 2). Agglomeration of Ag and TiO_2 increased twenty-one days after manufacturing. The large sized particles that were made by agglomeration were removed from analysis when the particles passed through a spray chamber. Consequently, the proportion of small sized particles increased fourteen days after manufacturing and the mean size of the sample decreased. The decrease of particle concentration over time was also due to the agglomeration of particles. As storage duration increased, the standard deviation also increased, and data became unstable. Therefore, it is recommended that sample analysis be performed as quickly as possible and not exceed one day for accurate size and particle concentration results. Therefore, all samples used in this study were analyzed in one day.

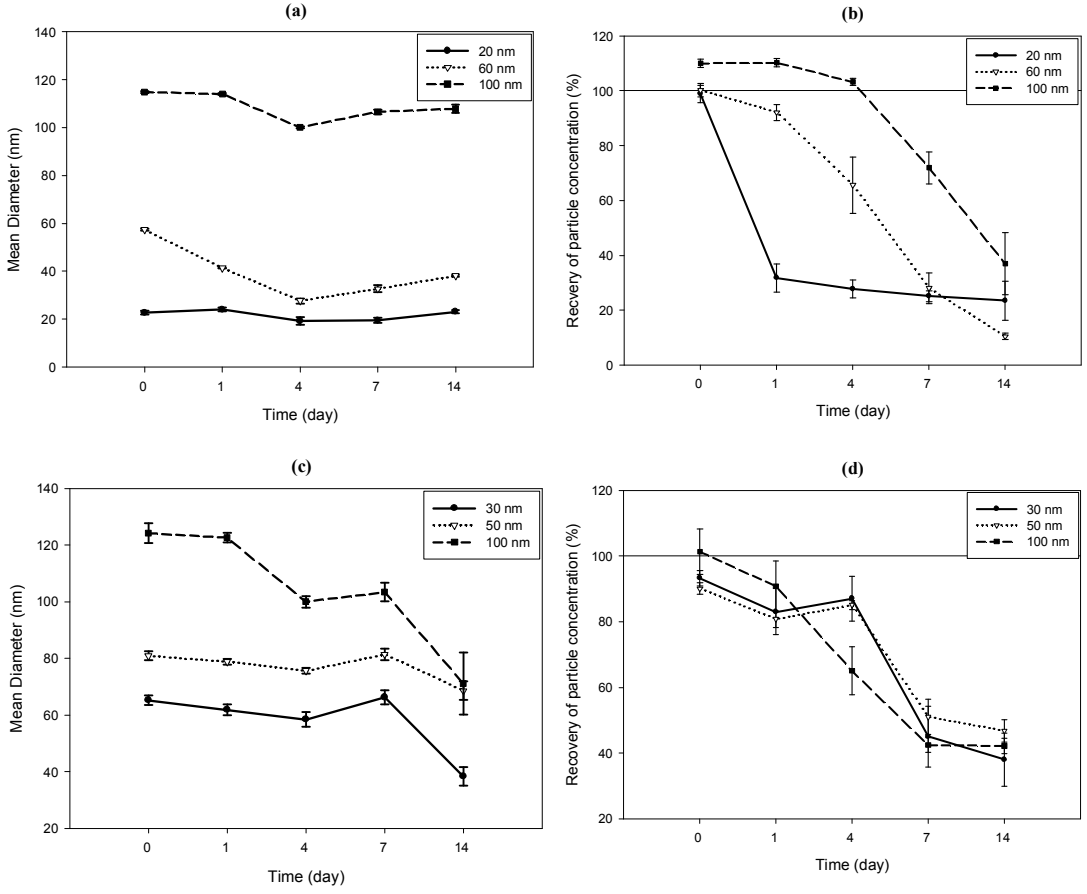

Figure 3. Variation of particle size and recovery over time. (a) Particle size variation of Ag (20, 60, and 100 nm). (b) Variation of recovery of particle concentrations of Ag (20, 60, and 100 nm). (c) Particle size variation of TiO_2 (30, 50, and 100 nm). (d) Variation of recovery of particle concentration of TiO_2 (30, 50, and 100 nm).

3.1.2. Accuracy and precision

Ag and TiO_2 reagents were analyzed using TEM to confirm their size and shape; these results were compared with SP-ICP-MS data. The size distribution of Ag reagents was matched with the manufacturer-claimed information (20 nm ± 4 nm, 60 nm ± 8 nm, 100 nm ± 8 nm). The size distribution of TiO_2 reagents, which were not provided from a manufacturer, had a wide range of sizes (Appendix 3). TiO_2 nanoparticle reagents used in this study showed multiple size distributions. Size accuracy using SP-ICP-MS was evaluated using level 1 to 4 particle mass concentration samples (Table 2). Size accuracy data is shown in Table 4. Two types of size data were provided: most frequent size and mean size. The most frequent sizes of Ag and TiO_2 particles were under the method detection limit (Ag: 16.9 nm and TiO_2: 24.4 nm). The mean size accuracy of Ag was 96 – 107%, and the SD was lower than TiO_2. The mean size accuracy of Ag increased with increasing size (20 nm: 80.2%; 60 nm: 87.09%; 100 nm: 59.01%). The mean size accuracy of 30 nm and 60 nm TiO_2 particles was 121 – 237%, and the mean size accuracy of 100 nm TiO_2 was 97 – 115%. The most frequent size was smaller than the mean size, but it matched the size distribution acquired from TEM analysis. The mean size corresponded with the average size provided by the manufacturer. Therefore, the mean size was appropriately used to evaluate the size accuracy rather than the most frequent size.

Before calculating the recovery of particle concentration, a calibration curve was prepared for each size of Ag and TiO_2 particles ($R^2 > 0.99$) (Appendix 4).

The recovery of particle concentration was in an acceptable range, Ag: 91 – 105% and TiO_2: 91 – 109%, except for the level 1 concentration of 30 nm TiO_2 (133%) (Table 4 and Figure 4). A significant tendency of recovery was not observed for Ag and TiO_2. The pooled RSD of TiO_2, 30 nm: 4.67; 60 nm: 6.41; 100 nm: 5.78, was slightly higher than the pooled RSD of Ag, 20 nm: 4.88; 60 nm: 3.85; 100 nm: 4.69. Ag provided more stable data than TiO_2 according to SD and pooled RSD values. Recovery of particle concentration was in an acceptable range for both Ag and TiO_2.

Precision was evaluated using RSD on six data items (most frequent size, mean size, mean intensity, particle concentration, dissolved intensity, and dissolved concentration). Precision data is shown in Table 5. The average RSD value of all data items was under 3 for both Ag and TiO_2, except for the most frequent size of TiO_2. Overall RSD values of TiO_2 were slightly higher than the overall RSD values of Ag. In particular, the RSD value for the most frequent sized TiO_2 was very high, 0.18 – 106.88. The lowest RSD values were the RSDs of dissolved concentrations (Ag: 0.09-3.41 and TiO_2: 0.01-0.65). Stable data on mean size, mean intensity, particle concentration, dissolved intensity, and dissolved concentration were obtained; stable data was not obtained on the most frequently sized item. In summary, Ag and TiO_2 analysis provided stable data for all data items except the most frequent size data.

Table 4. Size accuracy and recovery of particle concentration for each size of Ag and TiO_2

Substance	Particle size (nm)	N	Particle mass concentration (ppb)	Most Freq. Size (nm)	Most Freq. Size accuracy[1)] (%)	Mean Size (nm)	Mean Size accuracy (%)	Recovery of particle mass concentration (%)
Ag	20	3	0.002	<MDL[2)]	<MDL	19.3±0.4	96.6±1.9	103.1±4.8
		3	0.003	<MDL	<MDL	19.8±0.3	99.2±0.2	105.3±5.1
		3	0.004	17.4±0.3	86.9±1.3	20.2±0.1	101.2±0.9	98.6±6.0
		3	0.007	<MDL	<MDL	19.2±0.2	95.9±0.8	99.5±7.8
	Subtotal	12		<MDL	-	19.6±0.5	98.2±3.7	101.3±6.5
	60	3	0.048	52.7±4.9	87.9±8.1	59.6±3.6	99.3±6.0	99.7±3.3
		3	0.077	51.6±2.4	85.9±4.0	59.5±2.3	99.2±3.8	101.4±3.6
		3	0.096	52.3±4.3	87.2±7.2	61.5±3.2	102.5±5.4	105.3±6.0
		3	0.192	52.4±1.9	87.4±3.2	63.5±0.5	105.8±0.9	95.0±5.4
	Subtotal	12		52.3±4.7	87.1±7.8	61.0±4.6	101.7±7.7	99.6±5.2
	100	3	0.188	84.0±5.6	84.0±5.6	99.4±6.8	99.4±6.8	97.7±6.9
		3	0.313	92.5±8.1	92.5±8.1	98.0±8.7	98.0±8.7	97.9±4.3
		3	0.376	92.0±4.5	92.0±4.5	107.2±5.0	107.2±5.0	91.9±3.7
		3	0.752	87.6±8.9	87.6±8.9	101.7±8.1	101.7±8.1	91.0±6.2
	Subtotal	12		89.0±6.9	89.0±6.9	101.6±8.0	101.6±8.0	94.5±6.3
TiO_2	30	3	0.02	<MDL	<MDL	71.4±2.8	237.5±9.4	133.2±4.1
		3	0.10	<MDL	<MDL	69.8±2.6	231.8±8.6	108.9±9.2
		3	0.20	<MDL	<MDL	64.9±1.9	216.9±6.3	92.5±4.7
		3	0.25	26.3±13.0	95.4±43.4	71.0±3.4	236.7±11.3	99.2±4.8
	Subtotal	12		<MDL	-	68.7±3.4	229.1±11.5	106.3±15.8
	50	3	0.33	<MDL	<MDL	59.5±10.2	121.8±20.3	91.5±9.3
		3	1.00	<MDL	<MDL	76.9±4.2	153.5±8.3	90.1±4.1
		3	1.67	<MDL	<MDL	75.7±2.8	150.5±5.7	96.6±6.1
		3	2.50	<MDL	<MDL	75.7±3.4	149.2±6.8	98.8±8.9
	Subtotal	12		<MDL	-	72.0±8.6	144.1±17.2	94.7±8.0
	100 nm	3	10.00	<MDL	<MDL	97.3±1.9	97.3±1.9	106.3±8.6
		3	16.67	48.6±23.0	48.6±23.0	106.5±9.4	106.5±9.4	96.1±8.1
		3	20.00	<MDL	<MDL	107.4±6.7	107.4±6.7	103.3±7.6
		3	25.00	33.2±10.3	33.2±10.3	115.5±1.4	115.5±1.4	90.7±2.9
	Subtotal	12		<MDL	-	106.4±8.7	106.4±8.7	100.6±9.4

[1)]Size accuracy (%) = Detected size/Spiked size * 100
[2)]Method detection limit (Ag: 16.9 nm and TiO_2: 24.4 nm).

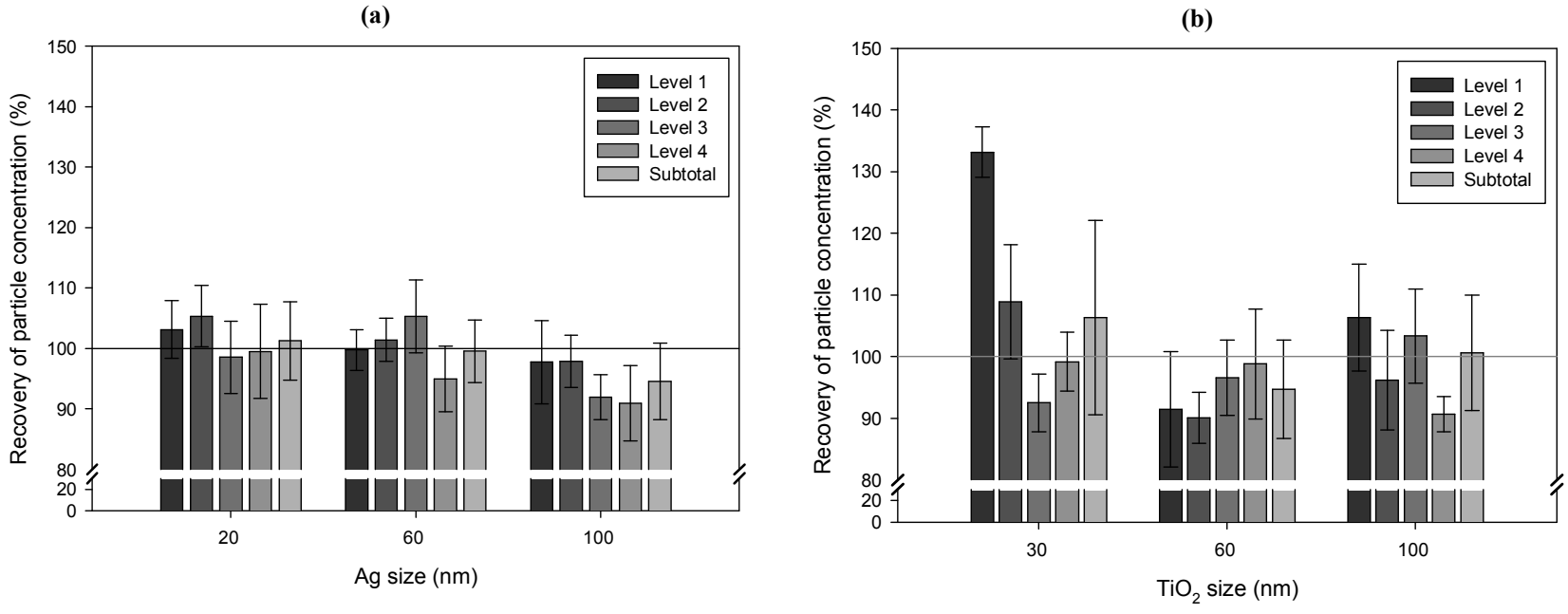

Figure 4. Recovery of particle concentration for each concentration level and size of (a) Ag and (b) TiO_2. Particle concentration was not directly presented because the concentration was differed according to the Ag or TiO_2 and particle size as seen in Table 4.

Table 5. RSD (%) for each data type of Ag and TiO_2 (n=12)

Substance	Data classification	RSD AM±SD	Range of RSD
Ag	Most Frequent. Size	1.19±1.89	0.09 ~ 6.21
	Mean Size	1.30±1.78	0.06 ~ 5.64
	Mean Intensity	1.53±0.88	0.17 ~ 4.76
	Particle Concentration	1.46±1.27	0.07 ~ 5.79
	Dissolved Intensity	1.48±1.17	0.27 ~ 5.68
	Dissolved Concentration	1.19±1.06	0.09 ~ 3.41
TiO_2	Most Frequent. Size	19.10±25.46	0.18 ~ 106.88
	Mean Size	2.04±0.96	0.39 ~ 5.32
	Mean Intensity	2.91±1.42	0.82 ~ 8.14
	Particle Concentration	2.18±0.80	0.49 ~ 3.53
	Dissolved Intensity	1.61±0.82	0.07 ~ 3.66
	Dissolved Concentration	0.14±0.14	0.01 ~ 0.65

3.1.3. Size mixture

Recovery of particle concentration was in the acceptable range for samples containing a single sized particle (Table 4); however, in samples containing particles of mixed sizes, the recovery of particle concentration exhibited a different pattern (Figure 5). The recovery of Ag particles slightly decreased as the particle concentration increased; in contrast, the recovery of TiO_2 did not show any such tendencies. In samples containing Ag nanoparticles of mixed sizes, the recovery of the smallest sized particles (20 nm) was very low (18% - 37%), the recovery of the largest sized particles (100 nm) was very large (162% - 169%), and the recovery of the medium sized particles (60 nm) was modest (81% - 116%). The recovery of Ag particles increased as particle size increased, but recovery was slightly lower in high concentrations than in low concentrations. The recovery of TiO_2 from samples containing mixed sizes of TiO_2 particles was not more complicated than the recovery of Ag from samples containing mixed sizes of Ag particles. The recovery of 30 nm and 50 nm sized TiO_2 particles ranged from 29 to 49% and 26 to 45%, respectively; the recovery did not increase or decrease with variations in the concentration. The recovery of 100 nm sized TiO_2 particles ranged from 98 to 139% with a higher recovery obtained at high concentrations.

Mixed size samples were expected to exhibit trimodal distribution because single size samples exhibited unimodal size distribution. However, mixed size samples of Ag exhibited bimodal distribution, and mixed size samples of TiO_2 exhibited unimodal distribution (Figure 6). In samples containing mixed sizes of

Ag particles, the peak corresponding to 20 nm particles disappeared, the peak corresponding to 50 nm particles moved slightly to a larger size, and the peak corresponding to 100 nm particles did not vary much. The total recovery of Ag particles from mixed size samples was 91% to 112%. The bimodal distribution exhibited by samples containing a mixture of three differently sized Ag particles can be explained by an overlapping of widening peaks corresponding to the 20 and 60 nm particles and by the agglomeration of small sized Ag particles. In samples containing mixed sizes of TiO_2 particles, a relatively flat distribution was observed over the entire size range. Peaks of mixture and each size was less than peak of 20 nm and peaks were not changed much regardless of tested particle sizes. The total recovery of TiO_2 particles from mixed size samples was 55% to 69%. The most frequent particle size recovered with single mode was approximately 20 nm regardless of the particle size tested (Table 4).

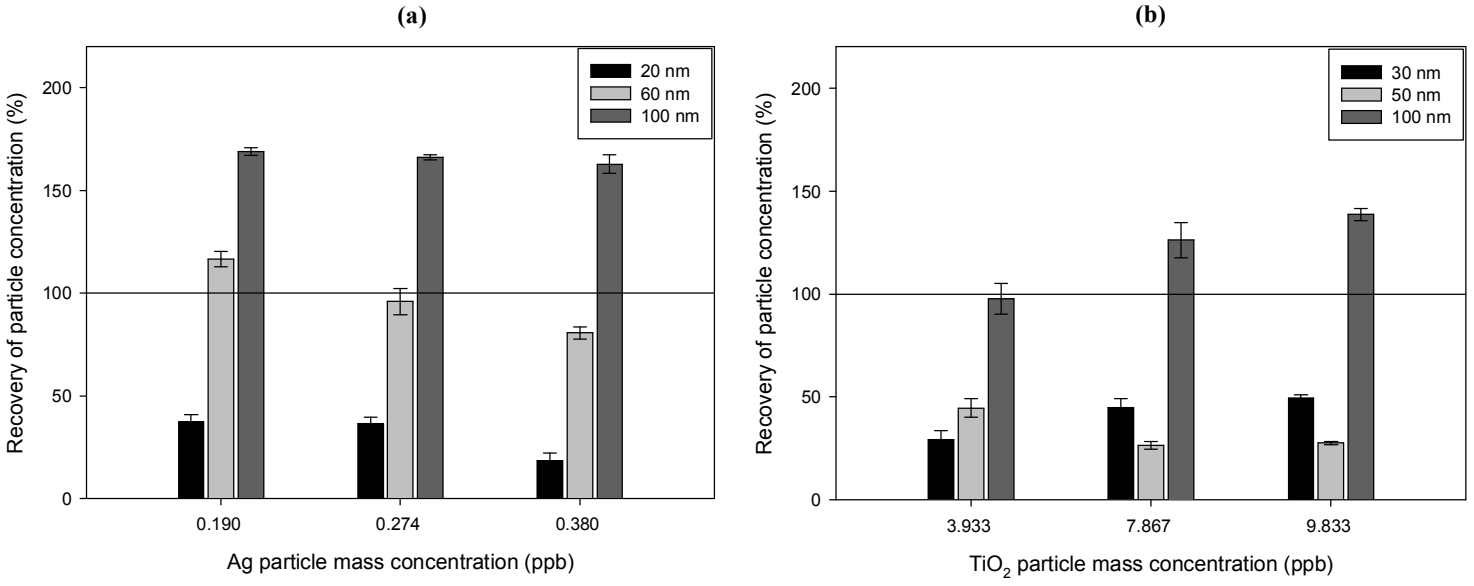

Figure 5. Recovery of particle concentrations for each concentration level of (a) Ag and (b) TiO_2 particles from mixed sized samples.

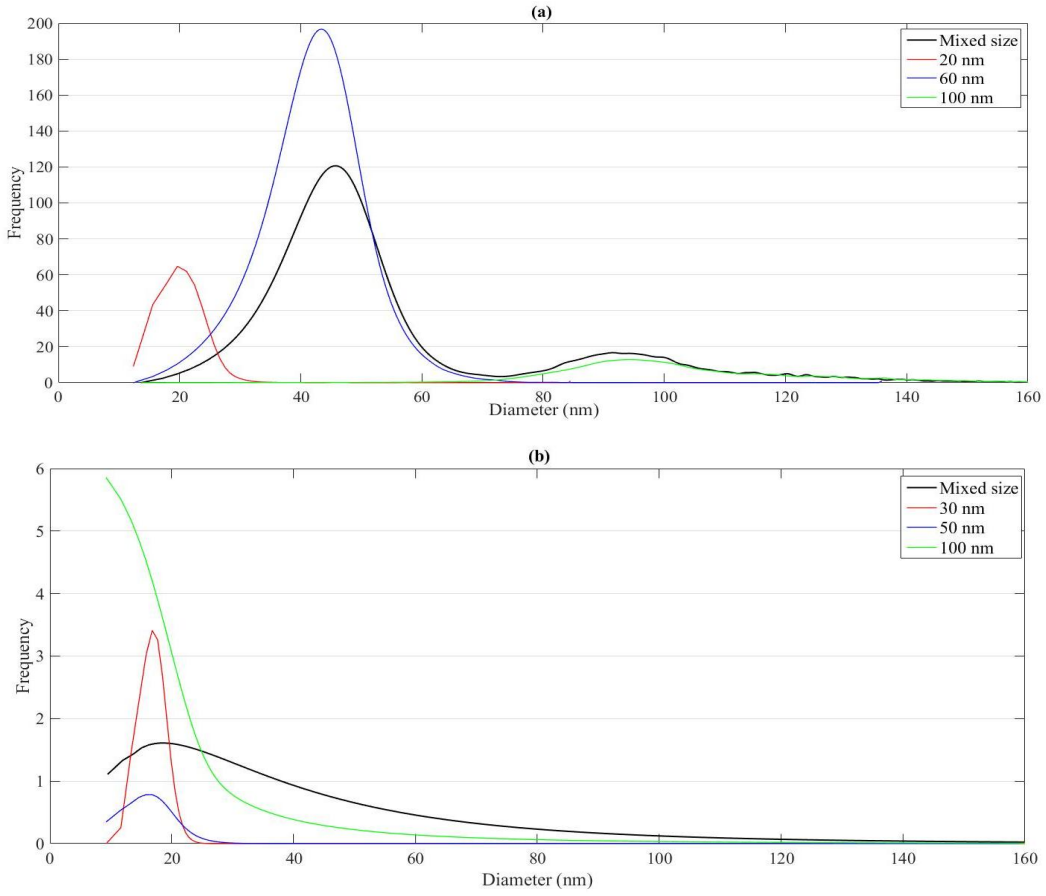

Figure 6. Size distribution of single and mixed samples of Ag and TiO_2. (a) Single size of 20, 60, and 100 nm Ag and mixed size (20, 60, and 100 nm) sample distribution of Ag. (b) Single size of 30, 50, and 100 nm TiO_2 and mixed size (30, 50, and 100 nm) sample distribution of TiO_2..

3.2. Consumer product samples

3.2.1. Comparison of pretreatment methods

To select an appropriate pretreatment method, 0.313 ppb of 100 nm Ag and 20 ppb of 100 nm TiO_2 were spiked in each type of solution media. The best pretreatment method was selected on the basis of particle size accuracy, particle concentration, and RSD values as seen in Table 6.

For Ag analysis, the optimal pretreatment methods included 0.1% of Tween 80 in both water and ethanol evaporation types of solution media. In the water type of solution media, the other methods were shown to decrease the size value and recovery of particle concentration compared with the DI pretreatment method (Table 6). Adding 0.1% of Tween 80 in the water type of solution media resulted in particles with a mean size of 106.9 nm, 95.6% of recovery, and a 1.85 RSD value. In experiments in an ethanol evaporation type of solution media, adding 0.1% of Tween 80 resulted in particles with a mean size of 91.1 nm, 93.8% recovery, and a 2.28 RSD value. Adding sonication methods were shown any tendency of data.

In TiO_2 analysis, the optimal pretreatment methods involved adding 0.1% of Triton X-100 in the water type of solution media and adding 0.1% of Tween 80 in the ethanol type of solution media. Using the optimal pretreatment method in the water type of solution media resulted in particles with a mean size of 111.6 nm, 94.5% of recovery, and a 5.84 RSD value. Using the optimal pretreatment method in the ethanol type of solution media resulted in particles with a mean size of 123.1

nm, 97.1% of recovery, and a 4.38 RSD value. In both the water and ethanol types of solution media, adding sonication decreased the particles' mean size and increased the recovery of particle concentration. In the ethanol evaporation type of solution media, adding sonication did not have any particular effects.

In Ag analysis, the Tween 80 method was the optimal method in water and ethanol evaporation types of bases. In TiO_2 analysis, the Triton X-100 method was the optimal method in the water type of base; the Tween 80 method was optimal in the ethanol type of base.

Table 6. Particle size and recovery of particle concentration in each pretreatment method of Ag (100 nm, 0.313 ppb) and TiO_2 (100 nm, 20 ppb)

Substance	Solution media	Pretreatment	Most Freq. Size (nm)	Mean Size (nm)	Recovery of particle mass concentration (%)	RSD[1] (%)
Ag	Water	DI[2]	77.3±3.2	99.0±3.2	81.1±6.8	8.38
		DI+S[3]	77.0±3.0	99.3±2.9	93.7±7.9	8.37
		Triton-X 100	82.0±0.6	106.5±1.8	103.7±6.3	6.03
		Triton-X 100+S	77.2±5.3	100.8±6.4	102.9±7.3	7.09
		Tween 80	81.6±1.2	106.9±1.6	98.6±1.8	1.85
		Tween 80+S	80.9±0.8	105.8±1.6	98.4±2.2	2.27
	Ethanol	DI	70.9±0.4	93.7±0.7	106.1±2.4	2.30
		DI+S	71.2±0.7	91.1±2.2	95.1±6.0	6.34
		Triton-X 100	63.9±0.6	84.7±0.7	100.0±10.6	10.63
		Triton-X 100+S	65.3±1.6	85.5±1.9	101.9±3.0	2.91
		Tween 80	62.8±1.5	83.8±0.9	101.2±3.6	3.58
		Tween 80+S	66.0±0.9	85.7±0.7	102.6±4.9	4.79
	Ethanol evaporation	DI	67.8±5.6	90.6±4.1	104.8±2.5	2.35
		DI+S	74.7±1.5	95.6±1.7	111.4±2.6	2.30
		Triton-X 100	70.4±1.5	88.6±1.1	87.1±1.9	2.12
		Triton-X 100+S	72.8±0.8	91.9±1.6	75.0±4.3	5.78
		Tween 80	72.6±1.9	91.1±2.3	96.8±2.2	2.28
		Tween 80+S	72.8±0.8	91.2±1.0	98.2±5.5	5.63
TiO_2	Water	DI	<MDL[4]	117.1±3.2	92.0±5.5	6.00
		DI+S	<MDL	114.7±2.5	110.5±6.0	5.45
		Triton-X 100	<MDL	111.6±2.8	94.5±5.5	5.84
		Triton-X 100+S	<MDL	116.8±4.2	94.3±5.4	5.69
		Tween 80	<MDL	119.0±1.5	108.3±5.0	4.64
		Tween 80+S	<MDL	119.5±2.2	112.0±4.0	3.55
	Ethanol	DI	63.1±8.9	128.6±1.7	123.1±7.9	6.44
		DI+S	67.5±11.5	125.3±2.8	125.1±6.0	4.76
		Triton-X 100	73.8±16.5	124.4±1.4	91.9±5.1	5.60
		Triton-X 100+S	69.9±9.1	121.9±3.8	120.8±8.0	6.58
		Tween 80	62.6±6.3	123.1±2.5	97.1±4.3	4.38
		Tween 80+S	69.5±8.7	124.4±1.4	100.0±5.3	5.34
	Ethanol evaporation	DI	64.2±7.0	125.6±3.2	122.8±23.1	18.79
		DI+S	73.4±8.4	123.3±1.8	104.6±12.8	12.26
		Triton-X 100	68.1±15.4	121.9±2.3	112.4±11.6	10.29
		Triton-X 100+S	67.2±10.9	128.4±2.5	127.4±3.5	2.74
		Tween 80	73.3±8.8	122.7±1.9	126.1±17.5	13.92
		Tween 80+S	72.7±9.3	128.5±1.5	140.6±6.0	4.27

[1]RSD of particle mass concentration
[2]Double distilled water
[3]Sonication
[4]Method detection limit (Ag: 16.9 nm and TiO2: 24.4 nm).

3.2.2. Particle size and concentration of consumer products

The Tween 80 method was used with water and ethanol bases for Ag analysis of consumer product samples. Samples containing the ethanol type of solution media were evaporated at 80 °C for 15 minutes. For TiO_2 analysis of consumer product samples, the Triton X-100 method was applied to a water base, and the Tween 80 method was applied to an ethanol base. The lower size limit of detection of Ag particles was 16.9 nm, and the lower size limit of detection of TiO_2 particles was 24.4 nm. The upper size limit of detection was approximately 200 nm.

The particle sizes and particle number concentrations of consumer spray products A to J are summarized in Table 7. Generally, the sizes of Ag NPs in consumer spray products were larger than TiO_2 NPs, and the particle number concentration of Ag NPs was lower than the concentration of TiO_2 NPs. Most of the particles contained in consumer spray products were nanosized (72.85% to 100%). Although some consumer spray products had no labelling information about containing NPs, products contained Ag and TiO_2 NPs. The Ag ion concentration ranged from 3.7 to 21.7 ppb. Products A to C, which were labeled as containing Ag NPs, had higher concentrations (11 to 22 ppb) and higher mean sizes of particles (60 to 81 nm) compared with other products (concentration 3-10 ppb, mean size 27-38 nm). Product D, although labeled as containing Ag NPs, had a similar mean size of particles compared with products H to J, which had no labels indicating that they contained Ag NPs. Products E to G, which were labeled as containing TiO_2 NPs, had particles of similar size to the Ag NPs because the three products were

manufactured from the same company. All products had more than 4.0×10^5 Ag nanoparticles/mL. Even though products had no label about containing Ag NPs, products had similar particle number concentrations. Product H had the highest nanoparticle number concentration (3.9×10^7 particles/mL), and product C had the lowest nanoparticle number concentration (4.7×10^5 particles/mL). The particle number concentration of nanosized Ag particles (<100 nm) made up the majority of the particle number concentration (72.85% to 100%).

The TiO_2 nanoparticle concentration was over 7.0×10^7 particles/mL in products A, B, C, D, H, I, and J. Products E to G had labels stating that they contained TiO_2 NPs, but the NP sizes of products E, F, and G were over the upper size detection limit (approximately 200 nm). Products B, D, and J had particle concentrations lower than 10 ppb, and products A, C, H, and I had particle concentrations ranging from 13.1 ppb to 47.9 ppb. Overall, the products had particles in a similar size range (50.1 nm to 65.3 nm) except for product B (35.2 nm). Product B, which was labeled as containing Ag NPs, had the highest particle number concentration (9.2×10^8 particles/mL), and product A had the lowest particle number concentration (7.7×10^5 particles/mL). The percentage of total particles that were nanosized was 87.16% to 99.49.

Generally, the detected particle sizes corresponded with SP-ICP-MS results when the SEM and TEM results were combined. A representative SEM and TEM-EDX result from product E is shown in Figure 7. From SP-ICP-MS and TEM analysis, Ag NPs in product E were detected, and agglomerated TiO_2 particles were also detected from SEM and TEM images. From SP-ICP-MS and SEM analysis,

Ag and TiO_2 NPs in product B were detected, but only TiO_2 NPs in product B was detected (Appendix 5). Ag and TiO_2 NPs were not distinguished accurately by SEM-EDX analysis because of coated and aggregated particles with unknown ingredients such as product B,. TEM images of 8 other products are shown in Appendix 6.

Table 7. Particle size and particle number concentration of consumer spray products (AM±SD, N=3)

Analyte	Product	Most frequent size (nm)	Mean Size (nm)	Dissolved ion concentration (ppb)	Particle number concentration (#/ml)		Particle number concentration percentage (%)		RSD[1] (%)
					<100 nm	>100 nm	<100 nm	>100 nm	
Ag[2]	A	40.8±0.1	59.5±0.3	10.7±0.0	1.3×10^6	1.1×10^5	92.37	7.63	3.54
	B	56.5±0.4	63.4±0.3	21.1±0.0	1.1×10^7	1.2×10^5	98.90	1.10	2.68
	C	51.6±0.4	80.8±1.6	21.7±0.0	4.7×10^5	1.8×10^5	72.85	27.15	3.34
	D	19.1±2.0	27.8±0.2	4.0±0.0	3.0×10^7	1.1×10^4	99.96	0.04	2.10
	E	31.8±0.5	37.3±0.8	7.7±0.0	5.1×10^6	4.8×10^3	99.90	0.10	3.73
	F	32.8±1.0	38.3±0.6	9.6±0.0	3.8×10^6	4.6×10^3	99.88	0.12	3.64
	G	31.2±0.4	36.4±0.1	7.7±0.0	4.2×10^6	2.3×10^3	99.94	0.06	2.06
	H	17.9±0.0	26.5±0.1	3.7±0.0	3.9×10^7	5.8×10^3	99.98	0.02	2.35
	I	17.9±0.0	26.8±0.1	3.9±0.0	2.6×10^7	2.9×10^3	99.99	0.01	0.86
	J	19.8±0.0	28.0±0.1	3.8±0.0	2.6×10^7	0	100.00	0.00	2.33
TiO_2[3]	A	36.4±0.6	65.3±0.1	47.9±0.1	7.8×10^7	1.8×10^7	87.16	12.84	5.30
	B	<MDL[4]	35.2±1.1	3.3±0.0	9.2×10^8	4.5×10^6	99.49	0.51	5.13
	C	32.1±0.8	55.6±0.5	22.3±0.2	2.6×10^8	1.2×10^7	95.75	4.25	10.86
	D	28.3±0.2	55.5±0.4	9.4±0.0	1.9×10^8	1.3×10^7	93.65	6.35	6.01
	E	>UDL[5]	>UDL	-	>UDL	>UDL	-	-	-
	F	>UDL	>UDL	-	>UDL	>UDL	-	-	-
	G	>UDL	>UDL	-	>UDL	>UDL	-	-	-
	H	31.9±1.2	57.4±1.0	16.9±0.2	2.2×10^8	1.2×10^7	94.73	5.27	4.86
	I	29.7±0.4	57.4±0.1	13.1±0.0	2.2×10^8	1.4×10^7	93.98	6.02	0.05
	J	25.4±0.5	50.7±1.1	5.1±0.0	1.7×10^8	8.3×10^6	95.42	4.58	1.64

[1] RSD of particle number concentration
[2] adding 0.1% Tween 80 at water base and adding 0.1% Tween 80 at ethanol evaporation base for Ag NP analysis
[3] adding 0.1% Triton X-100 at water base and adding 0.1% Tween 80 at ethanol base for TiO_2 NP analysis
[4] Method detection limit (Ag: 16.9 nm and TiO_2: 24.4 nm).
[5] Upper size detection limit

(a) (b)

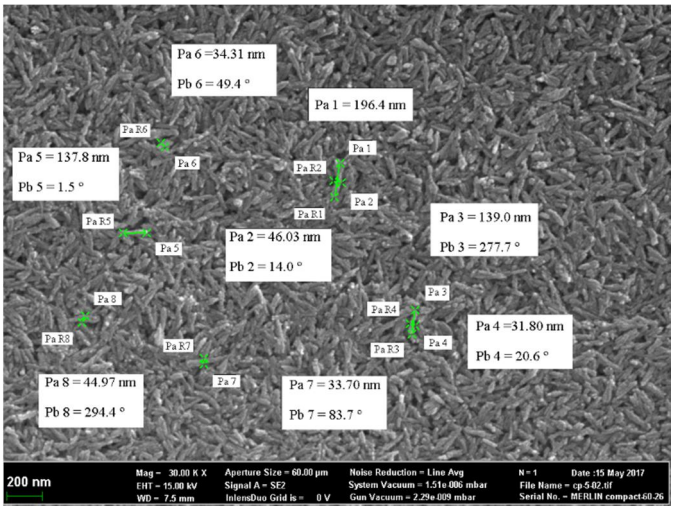

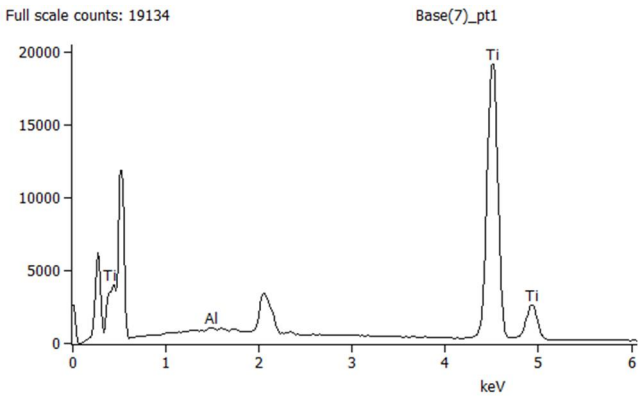

(c) (d)

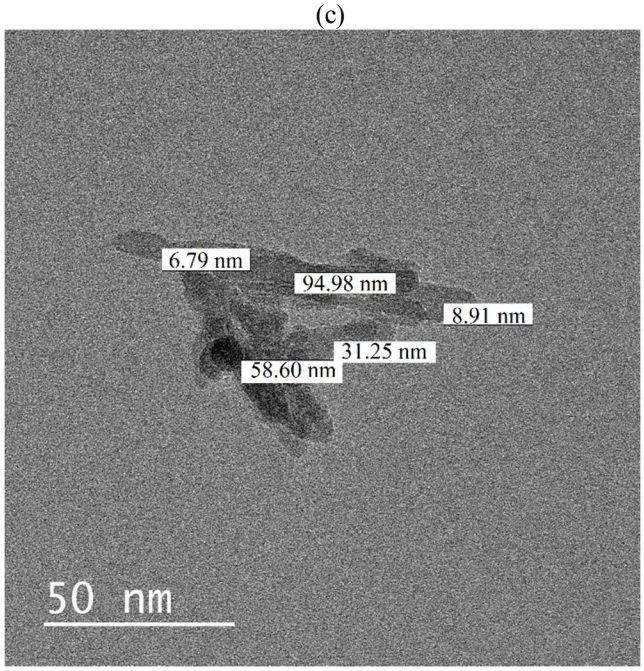

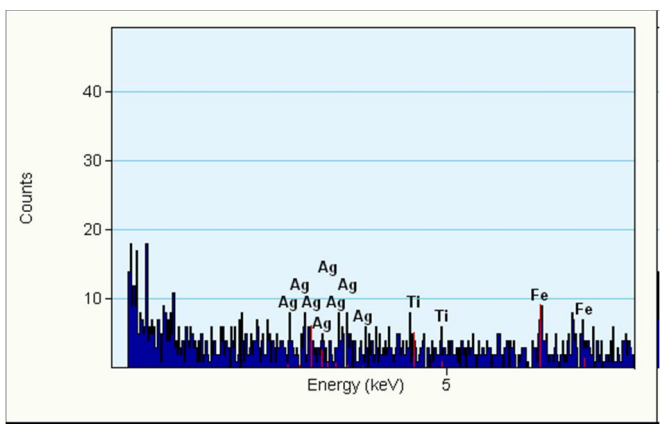

Figure 7. FE-SEM-EDS and TEM-EDS images of Product E. (a) FE-SEM-EDS image of product E (x30 k magnification) (b) FE-SEM-EDS spectra of product E (c) TEM-EDS image of product E (x50 magnification) (d) TEM-EDS spectra of product E.

4. Discussion

In this study, the use of SP-ICP-MS for analyzing nanoparticles was evaluated, and the evaluated method was used to analyze Ag and TiO_2 NPs in consumer spray products. To evaluate the SP-ICP-MS method, the following components were assessed: accuracy of particle size and particle concentration, precision of data, and stability. Experiments were performed using samples containing mixed sizes of particles. Consumer spray products were analyzed using an optimal pretreatment method.

The size accuracy of three sizes of Ag NPs was 96 to 107% (Table 4), and this result was similar to other studies (Kim et al., 2017; Pace et al., 2012; Peters et al., 2014). The size accuracy of three sizes of TiO_2 NPs was 97 to 237%. The size accuracy of 100 nm TiO_2 NPs (97 to 115%) was similar to other studies, but the sizes of 30 and 50 nm TiO_2 NPs were overestimated compared with other studies. In other studies, the size accuracy of TiO_2 was 97 to 123% (Vidmar et al., 2017). The sizes of TiO_2 NPs were overestimated because the reagents used in this study were made with multiple sizes of TiO_2 NPs, whereas TiO_2 nanoreagents used in the other study contained only a single size of TiO_2 NPs. The recovery of particle concentration of Ag and TiO_2 (91 to 109%, excluding 0.020 ppb of 30 nm TiO_2) was similar to other studies (Kim et al., 2017; Laborda et al., 2011; Peters et al., 2014; Vidmar et al., 2017). In this study, precision was better than previous studies. Precision was in an acceptable range in this study. The RSD value of mean size, particle concentration, and dissolved concentration was 0.14 to 2.18 (Table 5), and

the RSD value was 0.8 to 11.63 in other studies (Dan et al., 2015; Peters et al., 2015; Peters et al., 2015). The RSD value of the most frequent sized item in TiO_2 NP analysis was extremely high; the explanation for this was not identified.

Stability experiments showed reproducibility within one day after manufacturing. It is recommended to analyze samples as soon as possible after sample preparation to acquire the best data. The particle size and recovery decreased as the storage term was extended; this was similar to other studies (Peters et al., 2014; Witzler et al., 2016). After 2 weeks, the mean size accuracy of Ag particles in the sample ranged from 115 to 64%, and the mean size accuracy of TiO_2 particles in the sample ranged from 217 to 71% in this study (Figure 4). The percentage of decreased particle concentration were 73 to 90% in Ag analysis and 43 to 59% in TiO_2 analysis after 2 weeks.

Based on the size distribution and recovery of particle concentration when three particle sizes were mixed, the smaller size particles were agglomerated; hence, the bigger size recovery of particle concentration was increased. The smaller sized particles, 20 nm of Ag and 30 and 50 nm of TiO_2, showed 18 to 49% recovery of particle concentration. The bigger sized particles, 60 and 100 nm Ag and 100 nm of TiO_2, showed 81 to 169% recovery of particle concentration (Figure 5). The reason that recovery of particle concentration in samples containing mixed sizes was remarkably low was because the highest peak frequency value of the mixed size sample was lower and broader than those of the single size samples. The size distribution of samples containing three sizes of NPs was bimodal in Ag analysis

and unimodal in TiO_2 analysis (Figure 6). When differently sized particles were mixed, the peaks corresponding to 20 and 60 nm NPs coincided, resulting in a broadening of the width of the peak (Laborda et al., 2011).

The limit of detection (LOD) of this study was 16.86 nm (Ag) and 26.76 nm (TiO_2). This is a lower LOD than observed in other studies, 18 to 34 nm in Ag NP analysis (Laborda et al., 2011; Peters et al., 2015) and 50 to 100 nm in TiO_2 analysis (Degueldre et al., 2003; Peters et al., 2015). The upper size limit of detection was approximately 200 nm (Liu et al., 2014; Murphy et al., 2015). The detected sizes of NPs in consumer spray products were bigger than those reported in other studies. Cascio et al. (2015) reported Ag particles in 5 consumer products that ranged in size from 13 to 17 nm, whereas this study found Ag NPs in the range of 27 to 81 nm and TiO_2 NPs in the range of 35 to 65 nm (Table 6). The accuracy and precision differences of Ag and TiO_2 was due to the stability and characteristics of the reagents. Ag reagents were made as coated particles to minimize aggregation, but TiO_2 reagents were made as untreated powders.

Generally, the detected particle sizes and components corresponded with the SP-ICP-MS results when the SEM and TEM results were combined. In the case of coated and aggregated particles with unknown ingredients, such as product B, Ag and TiO_2 were not distinguished accurately by SEM-EDX analysis. In addition, the limit of detection of SEM and TEM is higher than SP-ICP-MS, so the SP-ICP-MS results could be different from the SEM and TEM results. Thus, when each particle cannot be distinguished and the particle concentration of sample is low,

SP-ICP-MS may be a more suitable method.

SP-ICP-MS is a promising analytical method to analyze metallic NPs and has a number of technical issues which have not been identified yet. Through this study, we confirmed the ability of SP-ICP-MS to accurately detect NP sizes and particle number concentrations. Using SP-ICP-MS, a suitable method is proposed to analyze various samples that have a similar matrix to consumer products. The results obtained from an analysis of consumer spray products are applicable to an exposure assessment of consumer products. With further method validation, the SP-ICP-MS method could characterize the particle size and particle number concentration of diverse samples.

Limitation

SP-ICP-MS analysis hypothesizes that target NPs have a spherical shape. If the target NP is not spherical, the results would not be exact. Therefore, combining SP-ICP-MS analysis with imaging techniques like electron microscopy is recommended.

The particle size and concentration was decreased after one day following manufacturing. Because the stability experiment was performed from one day to fourteen days after manufacture in this study, the exact storage term for stable data was not identified. To determine a storage period for stable analysis, a short-term stability experiment is needed. Furthermore, an additional study is needed to determine how to extend the storage period. In the stability and size mixture tests,

the reason for unpredictable recovery of particle concentration was not clearly identified. To investigate the reason, a particle mass concentration and dissolved metallic ion concentration matching experiment is required in further studies.

Because SP-ICP-MS can analyze only one target isotope at a time, the SP-ICP-MS method cannot distinguish between Ag NPs, Ag+ ions and other colloids such as AgCl. To improve the selectivity of SP-ICP-MS, a combination of various techniques such as Asymmetric Flow Field Fractionation has been studied.

So far, SP-ICP-MS is suitable for NPs that are bigger than ~ 20 nm. Because the limit of detection is determined by the sensitivity and detection efficiency of the instrument, an improvement of these factors in instruments is needed to analyze smaller sized NPs.

The results obtained showed that the optimal pretreatment method depended on the type of base and target analyte. Two types of dispersion media (Triton X-100 and Tween 80) affected the stability of the method. With further study, the reason should be established.

The instrumental parameter of TiO_2 analysis was set as rutile TiO_2. It is possible that the TiO_2 included in consumer spray products was anatase TiO_2 or a mixture of rutile and anatase TiO_2. This difference could decrease the accuracy of the results. For a more accurate analysis, classification of TiO_2 crystal phases is needed using X-ray Diffraction analysis.

SP-ICP-MS is a useful tool for examining inorganic colloidal materials that exist in

environmental samples (Pace et al., 2012). To control the variables, such as matrix effect, dwell time, sonication, dispersion medium, etc., further study is necessary.

5. Conclusions

This study provides a performance evaluation of a SP-ICP-MS method and its application to Ag and TiO_2 NP analysis of consumer spray products. This study shows that SP-ICP-MS is a viable method for analyzing NPs in consumer spray products.

Analysis of Ag NPs and bigger sized TiO_2 NPs provided reliable data, but analyses of smaller sized (<50 nm) TiO_2 NPs and mixed size samples were not reliable. It is recommended to analyze samples as quickly as possible, not to exceed one day, for accurate size and particle concentration data. Size mixture tests showed that poly size NP samples need a careful experimental design and data analysis.

All of the consumer spray products included Ag NPs, and eight of the consumer spray products included TiO_2 NPs according to SP-ICP-MS analysis. The Ag NP sizes in consumer spray products ranged from 27 to 81 nm, and the particle number concentration of Ag NPs was 4.7×10^5 to 3.9×10^7 particles/mL. The TiO_2 NP sizes in consumer spray products ranged from 35 to 65 nm, and the particle number concentration of TiO_2 NPs was $7.7 \times 10^7 - 9.2 \times 10^8$ particles/mL. The particle mass concentrations of Ag ranged from 0.002 to 0.129 ppb, and the particle mass concentrations of TiO_2 ranged from 2.122 to 7.140 ppb. The particle number concentrations of Ag and TiO_2 in consumer products were high, but the particle mass concentration was lower than 10 ppb because most of the particles in the consumer products were nanosized particles.

6. References

Azimi, P., Zhao, D., Pouzet, C., Crain, N. E., & Stephens, B. (2016). Emissions of ultrafine particles and volatile organic compounds from commercially available desktop three-dimensional printers with multiple filaments. Environmental science & technology, 50(3), 1260-1268.

Benn, T., Cavanagh, B., Hristovski, K., Posner, J. D., & Westerhoff, P. (2010). The release of nanosilver from consumer products used in the home. Journal of environmental quality, 39(6), 1875-1882.

Boxall, A. B., Tiede, K., & Chaudhry, Q. (2007). Engineered nanomaterials in soils and water: how do they behave and could they pose a risk to human health? Nanomedicine, 2(6), 919-927.

Calzolai, L., Gilliland, D., & Rossi, F. (2012). Measuring nanoparticles size distribution in food and consumer products: a review. Food Additives & Contaminants: Part A, 29(8), 1183-1193.

Choi, O., & Hu, Z. (2008). Size dependent and reactive oxygen species related nanosilver toxicity to nitrifying bacteria. Environmental science & technology, 42(12), 4583-4588.

Dan, Y., Shi, H., Stephan, C., & Liang, X. (2015). Rapid analysis of titanium dioxide nanoparticles in sunscreens using single particle inductively coupled plasma–mass spectrometry. Microchemical Journal, 122, 119-126.

Degueldre, C., & Favarger, P.-Y. (2003). Colloid analysis by single particle inductively coupled plasma-mass spectroscopy: a feasibility study. Colloids and Surfaces A: Physicochemical and Engineering Aspects, 217(1), 137-142.

Dudkiewicz, A., Wagner, S., Lehner, A., Chaudhry, Q., Pietravalle, S., Tiede, K., Grombe, R. (2015). A uniform measurement expression for cross method comparison of nanoparticle aggregate size distributions. Analyst, 140(15), 5257-

5267.

Fabian, E., Landsiedel, R., Ma-Hock, L., Wiench, K., Wohlleben, W., & Van Ravenzwaay, B. (2008). Tissue distribution and toxicity of intravenously administered titanium dioxide nanoparticles in rats. Archives of toxicology, 82(3), 151-157.

Foldbjerg, R., Olesen, P., Hougaard, M., Dang, D. A., Hoffmann, H. J., & Autrup, H. (2009). PVP-coated silver nanoparticles and silver ions induce reactive oxygen species, apoptosis and necrosis in THP-1 monocytes. Toxicology letters, 190(2), 156-162.

Gottschalk, F., Sonderer, T., Scholz, R. W., & Nowack, B. (2009). Modeled environmental concentrations of engineered nanomaterials (TiO_2, ZnO, Ag, CNT, fullerenes) for different regions. Environmental science & technology, 43(24), 9216-9222.

Hassellöv, M., Readman, J. W., Ranville, J. F., & Tiede, K. (2008). Nanoparticle analysis and characterization methodologies in environmental risk assessment of engineered nanoparticles. Ecotoxicology, 17(5), 344-361.

Hu, S., Liu, R., Zhang, S., Huang, Z., Xing, Z., & Zhang, X. (2009). A new strategy for highly sensitive immunoassay based on single-particle mode detection by inductively coupled plasma mass spectrometry. Journal of the American Society for Mass Spectrometry, 20(6), 1096-1103.

IARC Working Group on the Evaluation of Carcinogenic Risks to Humans. (2006). Cobalt in hard metals and cobalt sulfate, gallium arsenide, indium phosphide and vanadium pentoxide. IARC monographs on the evaluation of carcinogenic risks to humans, 86, 1.

Kennedy, E. R., Fischbach, T. J., Song, R., Eller, P. M., & Shulman, S. A. (1994). Guidelines for air sampling and analytical method development and evaluation (No. PB--95-241188/XAB). National Inst. for Occupational Safety and Health,

Cincinnati, OH (United States).

Kim, H.A., Lee, B.T., Na, S.Y., Kim, K.W., Ranville, J. F., Kim, S.O., Eom, I.C. (2017). Characterization of silver nanoparticle aggregates using single particle-inductively coupled plasma-mass spectrometry (spICP-MS). Chemosphere, 171, 468-475.

Klaine, S. J., Alvarez, P. J., Batley, G. E., Fernandes, T. F., Handy, R. D., Lyon, D. Y., Lead, J. R. (2008). Nanomaterials in the environment: behavior, fate, bioavailability, and effects. Environmental Toxicology and Chemistry, 27(9), 1825-1851.

Laborda, F., Jiménez-Lamana, J., Bolea, E., & Castillo, J. R. (2011). Selective identification, characterization and determination of dissolved silver (I) and silver nanoparticles based on single particle detection by inductively coupled plasma mass spectrometry. Journal of Analytical Atomic Spectrometry, 26(7), 1362-1371.

Lee, K., Trochimowicz, H., & Reinhardt, C. (1985). Pulmonary response of rats exposed to titanium dioxide (TiO_2) by inhalation for two years. Toxicology and applied pharmacology, 79(2), 179-192.

Liu, J., Murphy, K. E., MacCuspie, R. I., & Winchester, M. R. (2014). Capabilities of single particle inductively coupled plasma mass spectrometry for the size measurement of nanoparticles: a case study on gold nanoparticles. Analytical chemistry, 86(7), 3405-3414.

Lorenz, C., Windler, L., Von Goetz, N., Lehmann, R. P., Schuppler, M., Hungerbühler, K., & Nowack, B. (2012). Characterization of silver release from commercially available functional (nano) textiles. Chemosphere, 89(7), 817-824.

Losert, S., von Goetz, N., Bekker, C., Fransman, W., Wijnhoven, S. W., Delmaar, C., Ulrich, A. (2014). Human Exposure to Conventional and Nanoparticle-Containing Sprays: A Critical Review. Environmental science & technology, 48(10), 5366-5378.

Mahl, D., Diendorf, J., Meyer-Zaika, W., & Epple, M. (2011). Possibilities and limitations of different analytical methods for the size determination of a bimodal dispersion of metallic nanoparticles. Colloids and Surfaces A: Physicochemical and Engineering Aspects, 377(1), 386-392.

Murphy, K., Liu, J., Bustos, A. M., Johnson, M., & Winchester, M. (2015). Characterization of nanoparticle suspensions using single particle inductively coupled plasma mass spectrometry. NIST Special Publication, 1200, 21.

Nowack, B., Krug, H. F., & Height, M. (2011). 120 years of nanosilver history: implications for policy makers. Environmental science & technology, 45, 1177-1183.

Nowack, B., Ranville, J. F., Diamond, S., Gallego□Urrea, J. A., Metcalfe, C., Rose, J., Klaine, S. J. (2012). Potential scenarios for nanomaterial release and subsequent alteration in the environment. Environmental Toxicology and Chemistry, 31(1), 50-59.

Pace, H. E., Rogers, N. J., Jarolimek, C., Coleman, V. A., Gray, E. P., Higgins, C. P., & Ranville, J. F. (2012). Single particle inductively coupled plasma-mass spectrometry: a performance evaluation and method comparison in the determination of nanoparticle size. Environmental science & technology, 46(22), 12272-12280.

Peters, R., Herrera-Rivera, Z., Undas, A., van der Lee, M., Marvin, H., Bouwmeester, H., & Weigel, S. (2015). Single particle ICP-MS combined with a data evaluation tool as a routine technique for the analysis of nanoparticles in complex matrices. Journal of Analytical Atomic Spectrometry, 30(6), 1274-1285.

Peters, R. J., Rivera, Z. H., van Bemmel, G., Marvin, H. J., Weigel, S., & Bouwmeester, H. (2014). Development and validation of single particle ICP-MS for sizing and quantitative determination of nano-silver in chicken meat. Analytical and bioanalytical chemistry, 406(16), 3875-3885.

Quadros, M. E., & Marr, L. C. (2011). Silver nanoparticles and total aerosols emitted by nanotechnology-related consumer spray products. Environmental science & technology, 45(24), 10713-10719.

Quadros, M. E., Pierson IV, R., Tulve, N. S., Willis, R., Rogers, K., Thomas, T. A., & Marr, L. C. (2013). Release of silver from nanotechnology-based consumer products for children. Environmental science & technology, 47(15), 8894-8901.

Sapsford, K. E., Tyner, K. M., Dair, B. J., Deschamps, J. R., & Medintz, I. L. (2011). Analyzing nanomaterial bioconjugates: a review of current and emerging purification and characterization techniques. Analytical chemistry, 83(12), 4453-4488.

Shakeel, M., Jabeen, F., Shabbir, S., Asghar, M. S., Khan, M. S., & Chaudhry, A. S. (2016). Toxicity of Nano-Titanium Dioxide (TiO2. Biological trace element research, 172(1), 1-36.

Shi, H., Magaye, R., Castranova, V., & Zhao, J. (2013). Titanium dioxide nanoparticles: a review of current toxicological data. Particle and fibre toxicology, 10(1), 15.

Sklerov, J. H., & Couper, F. J. (2011). Calculation and verification of blood ethanol measurement uncertainty for headspace gas chromatography. Journal of analytical toxicology, 35(7), 402-410.

Stone, V., Hankin, S., Aitken, R., Aschberger, K., Baun, A., Christensen, F., & Johnston, H. (2010). Engineered nanoparticles: Review of health and environmental safety (ENRHES). Project final report. European Commission.

Vance, M. E., Kuiken, T., Vejerano, E. P., McGinnis, S. P., Hochella Jr, M. F., Rejeski, D., & Hull, M. S. (2015). Nanotechnology in the real world: Redeveloping the nanomaterial consumer products inventory. Beilstein journal of nanotechnology, 6(1), 1769-1780.

Vidmar, J., Milačič, R., & Ščančar, J. (2017). Sizing and simultaneous quantification of nanoscale titanium dioxide and a dissolved titanium form by single particle inductively coupled plasma mass spectrometry. Microchemical Journal, 132, 391-400.

Witzler, M., Küllmer, F., Hirtz, A., & Günther, K. (2016). Validation of Gold and Silver Nanoparticle Analysis in Fruit Juices by Single-Particle ICP-MS without Sample Pretreatment. Journal of agricultural and food chemistry, 64(20), 4165-4170.

국문초록

SP-ICP-MS를 이용한

나노물질 분석 방법 성능평가 및 응용

유단비

서울대학교 보건대학원

환경보건학과 산업보건전공

연구목적 : 나노 물질을 분석하는 다양한 분석 기법 중, 단일 입자 유도결합 플라즈마 질량 분석기 (SP-ICP-MS)는 낮은 농도에서도 분석이 가능한 점 등 나노 사이즈의 무기물 입자를 분석하기 위한 분석 기법으로써 새롭게 떠오르고 있다. 이 연구의 목적은 SP-ICP-MS를 이용해 수용액 시료에 포함되어 있는 나노 입자 분석 방법의 성능평가와 이를 이용한 생활화학제품 내 은과 이산화 티타늄 나노 입자 분석이다.

연구방법 : SP-ICP-MS 성능평가는 정확도, 정밀도, 시료 안정성, 다중 크기 입자 혼합시료에 대한 분석으로 이루어졌다. 정확도는 입자 크기 정확도와 입자 농도 회수율로 평가하였으며, 정밀도는 상대표준편차(RSD)와 통합표준편차로 평가하였다. 시료 안정성 실험은 제조일으로부

터 14일 동안 재 분석하여 결과값을 비교하였다. 생활화학제품 분석에 가장 적합한 전처리 방법을 확인하기 위해 3가지 베이스 (물, 에탄올, 에탄올 증발 베이스)별로 6가지 종류의 전처리 방법을 비교해 보았다. 총 10 종류의 생활화학 제품에 포함되어 있는 은 나노와 이산화 티타늄 나노를 분석하기 위해, 앞서 실험을 통해 가장 적합하다고 판단되는 전처리 방법을 적용한 SP-ICP-MS분석과 투사전자현미경과 주사전자현미경 분석이 이루어졌다.

연구결과 : SP-ICP-MS를 통한 은과 이산화 티타늄 분석의 정확도와 정밀도는 안정적이었다. 입자 크기 정확도는 30 nm와 50 nm 이산화 티타늄을 제외하고 그 외의 은과 이산화 티타늄의 경우 95-115%를 보였다. 입자농도 회수율은 가장 낮은 농도의 30 nm의 이산화 티타늄을 제외하고 91-109%를 보였다. 최빈도 입자크기 항목을 제외한 모든 항목에서 RSD 값은 0.01-6.21로 안정적인 값을 보였다. 은과 이산화 티타늄의 정확도와 안정성의 차이는 분석법 검증에 사용된 시약의 안정성과 정밀도의 차이에서 영향을 받은 것으로 보인다. 시료는 데이터의 질을 위해 제조 직후 분석하는 것을 추천한다. 여러 가지 크기의 입자가 혼합되어 있을 경우 큰 입자의 회수율을 100%를 넘었지만 작은 입자의 회수율은 50% 미만으로 응집 현상이 생기는 것으로 보여진다. 전처리 방법 별 비교를 통해 선정된 전처리 방법을 이용해 생활화학제품을 분석한 결과, 모든 제품에서 은 나노가, 8개 제품에서 이산화 티타늄 나노 입자

가 검출 되었다. 생활화학제품에 포함되어 있는 은 나노의 크기는 27–81 nm였으며, 은 나노 입자수 농도는 4.7×10^5–3.9×10^7 particles/ml였다. 생활화학제품에 포함되어 있는 이산화 티타늄 나노 입자의 크기는 35–65 nm였으며 입자 수 농도는 7.7×10^7–9.2×10^8 particles/ml였다. 또한 전자현미경 결과에서도 비슷한 입자의 성분과 크기를 보였다.

결론 : SP–ICP–MS는 새롭게 도입되고 있는 나노 입자 분석방법으로, 이에 대해 꾸준한 연구가 이루어 지고 있다. 이 연구를 통해서 은 나노 입자와 큰 사이즈의 이산화 티타늄 분석은 신뢰성 있는 결과를 제공하지만 작은 입자 (<50 nm)의 이산화 티타늄과 다중 크기의 시료 분석의 경우 적절하지 않다는 것을 알 수 있었다. 생활화학제품 분석 결과 모든 제품에서 은 나노가, 8개 제품에서 이산화 티타늄 나노 입자가 검출 되었으며, 입자 수 농도는 십만개 이상이었다. 생활화학제품 분석 결과는 생활화학제품을 통한 노출 평가 시에 활용 될 수 있을 것이다. 추후의 SP–ICP–MS 분석방법 확립에 대한 연구를 통해, 더욱 다양한 매질을 가진 시료에서 나노 입자 크기의 분석과 농도 분석이 가능해 질 것이다.

주요어: 단일 입자 유도 결합 플라즈마 질량 분석, 생활화학제품, 은, 이산화 티타늄, 분석법 성능평가, 나노 입자, 전처리

학번: 2015–24109

Appendix

Appendix 1. Three level of particle mass concentration for size mixture experiment

Substance	level	size (nm)	Particle mass concentration (ppb)
Ag	1	20	0.0010
		60	0.0320
		100	0.1567
		subtotal	0.1897
	2	20	0.0015
		60	0.0480
		100	0.2351
		subtotal	0.2846
	3	20	0.0021
		60	0.0639
		100	0.3135
		subtotal	0.3795
TiO_2	1	30	0.1000
		50	0.5000
		100	3.3333
		subtotal	3.9333
	2	30	0.2000
		50	1.0000
		100	6.6667
		subtotal	7.8667
	3	30	0.2500
		50	1.2500
		100	8.3333
		subtotal	9.8333

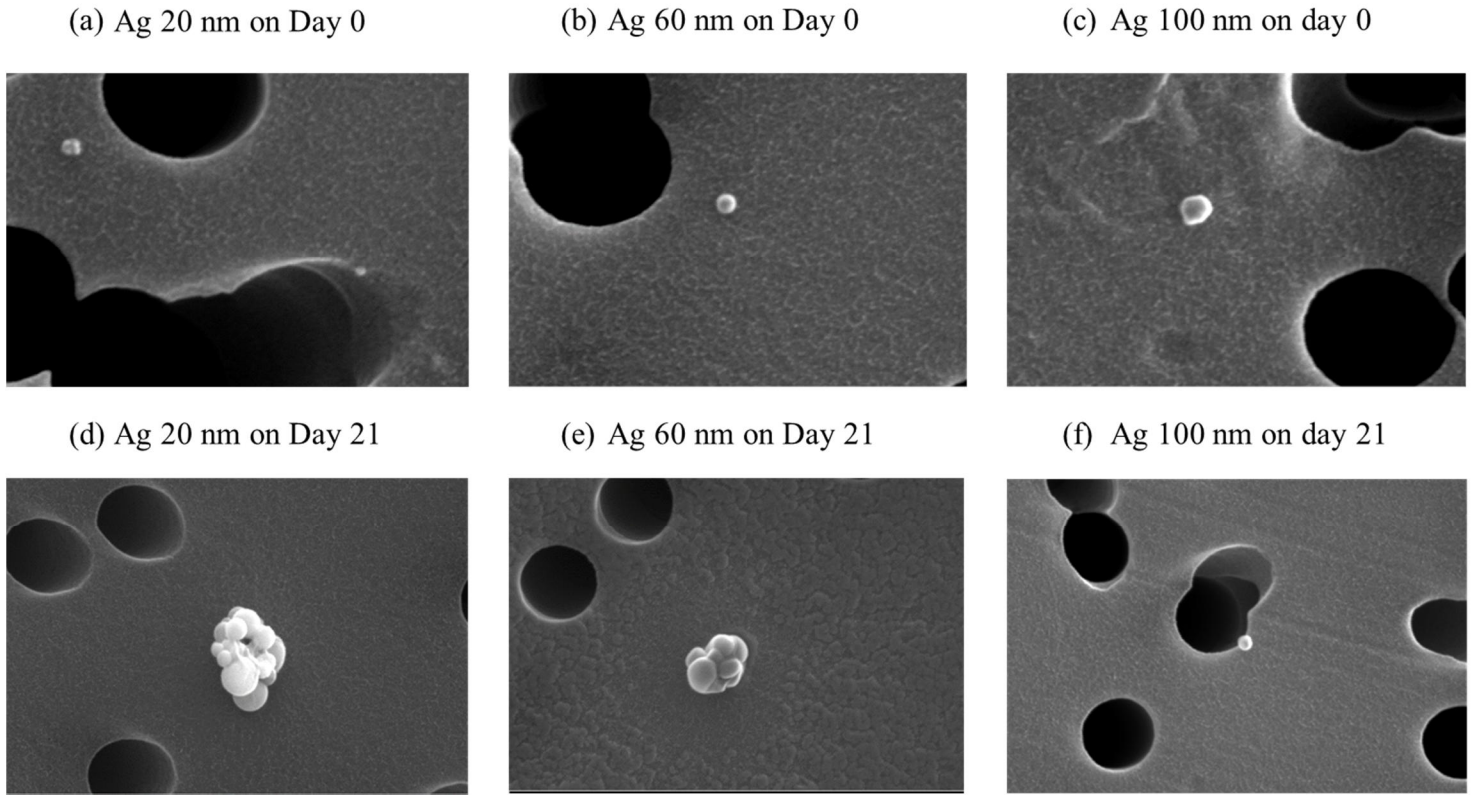

Appendix 2. FE-SEM-EDS image of Ag on day 0 and day 21. (a) 20 nm Ag on manufacturing day (x100k magnification) (b) 60 nm Ag on manufacturing day (x100k magnification) (c) 100 nm Ag on manufacturing day (x100k magnification) (d) 20 nm Ag at 21 days after manufacturing (x50k magnification) (e) 60 nm Ag at 21 days after manufacturing (x50k magnification) (f) 100 nm Ag at 21 days after manufacturing (x50k magnification)

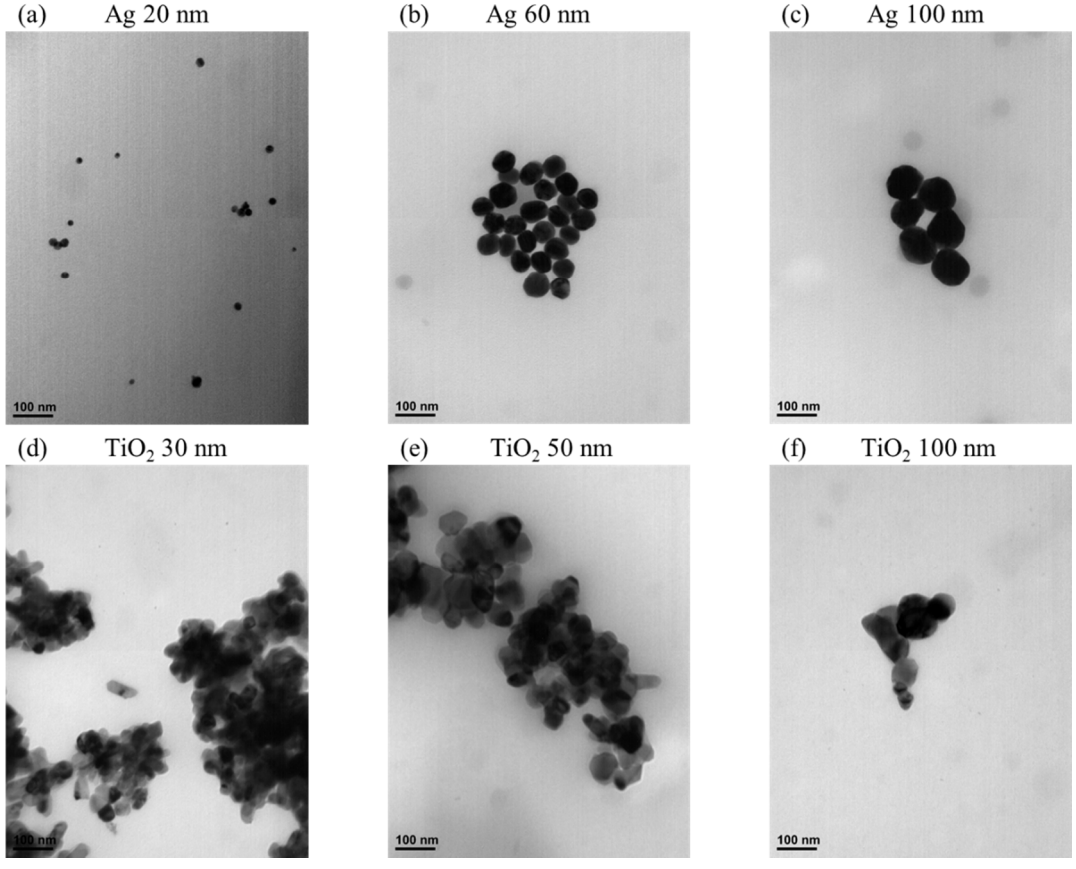

Appendix 3. TEM-EDS image of (a) 20 nm Ag, (b) 60 nm Ag, (c) 100 nm Ag, (d) 30 nm TiO_2, (e) 50 nm TiO_2, and (f) 100 nm TiO_2 (x200k magnification).

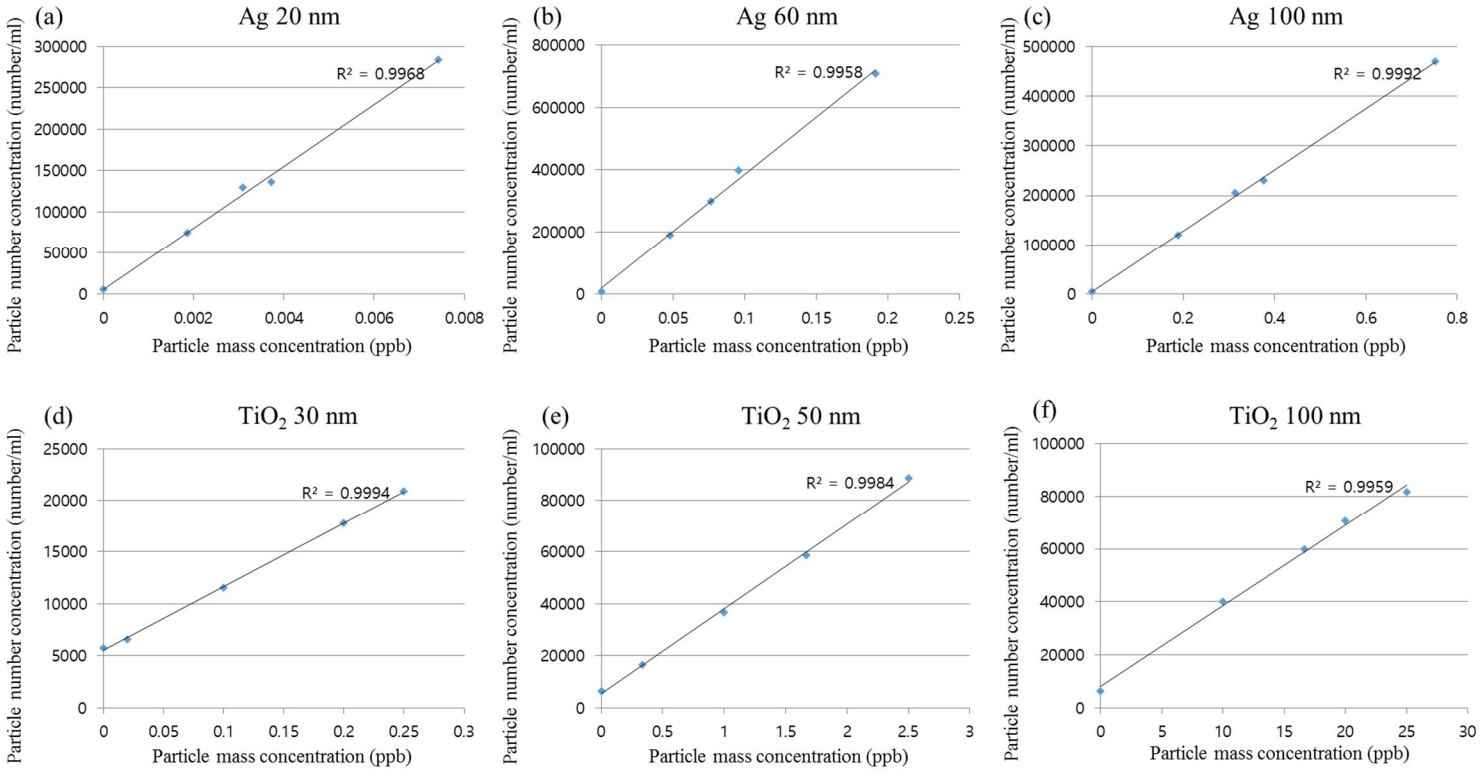

Appendix 4. Particle concentration calibration curve in each size of (a) 20 nm Ag, (b) 60 nm Ag, (c) 100 nm Ag, (d) 30 nm TiO_2, (e) 50 nm TiO_2, and (f) 100 nm TiO_2.

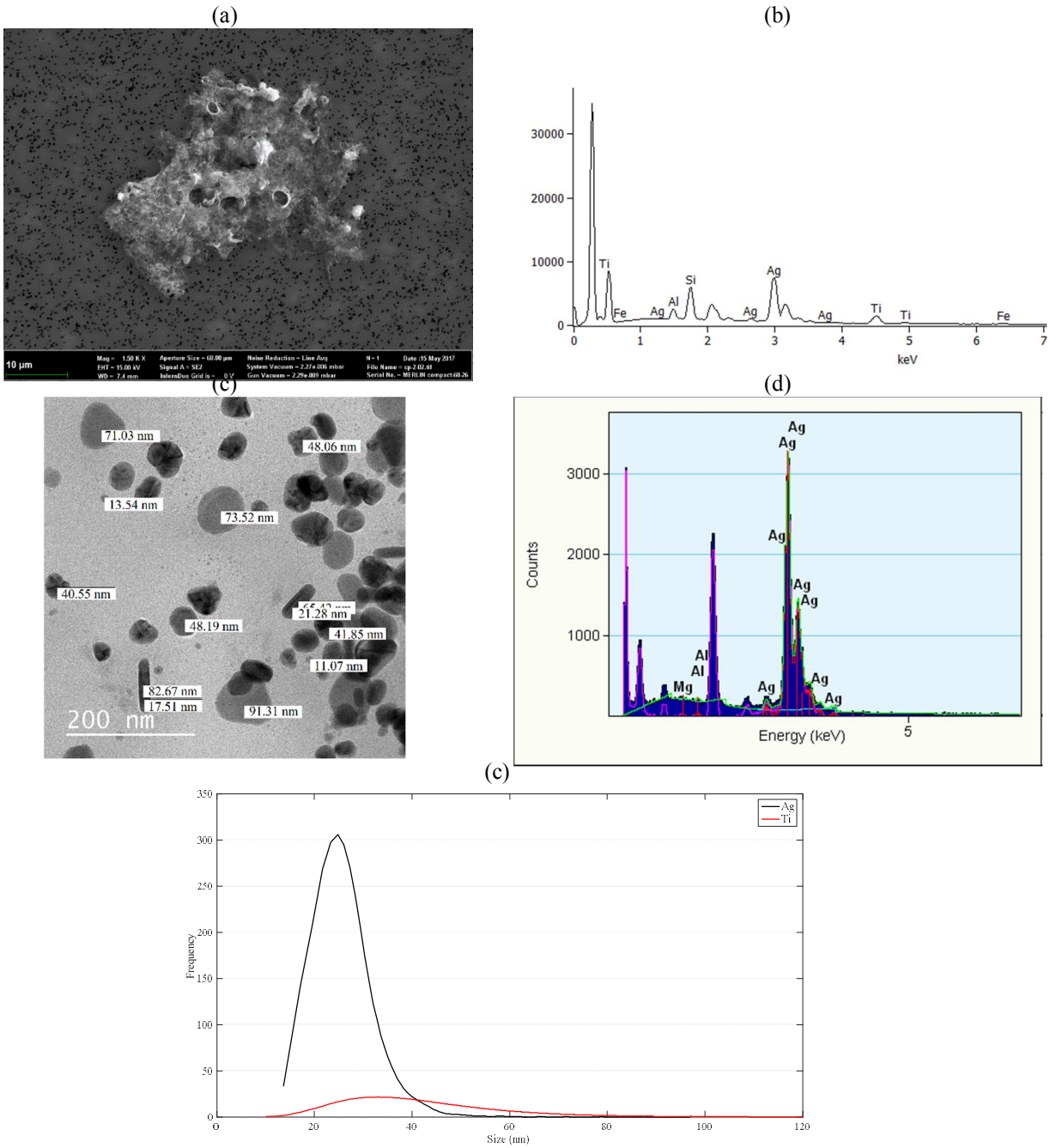

Appendix 5. FE-SEM-EDS and TEM-EDS image and size distribution of Product B. (a) FE-SEM-EDS image of product B (x1.5k magnification) (b) FE-SEM-EDS spectra of product B (c) TEM-EDS image of product B (x100 magnification) (d) TEM-EDS spectra of product B (e) size distribution of product B.

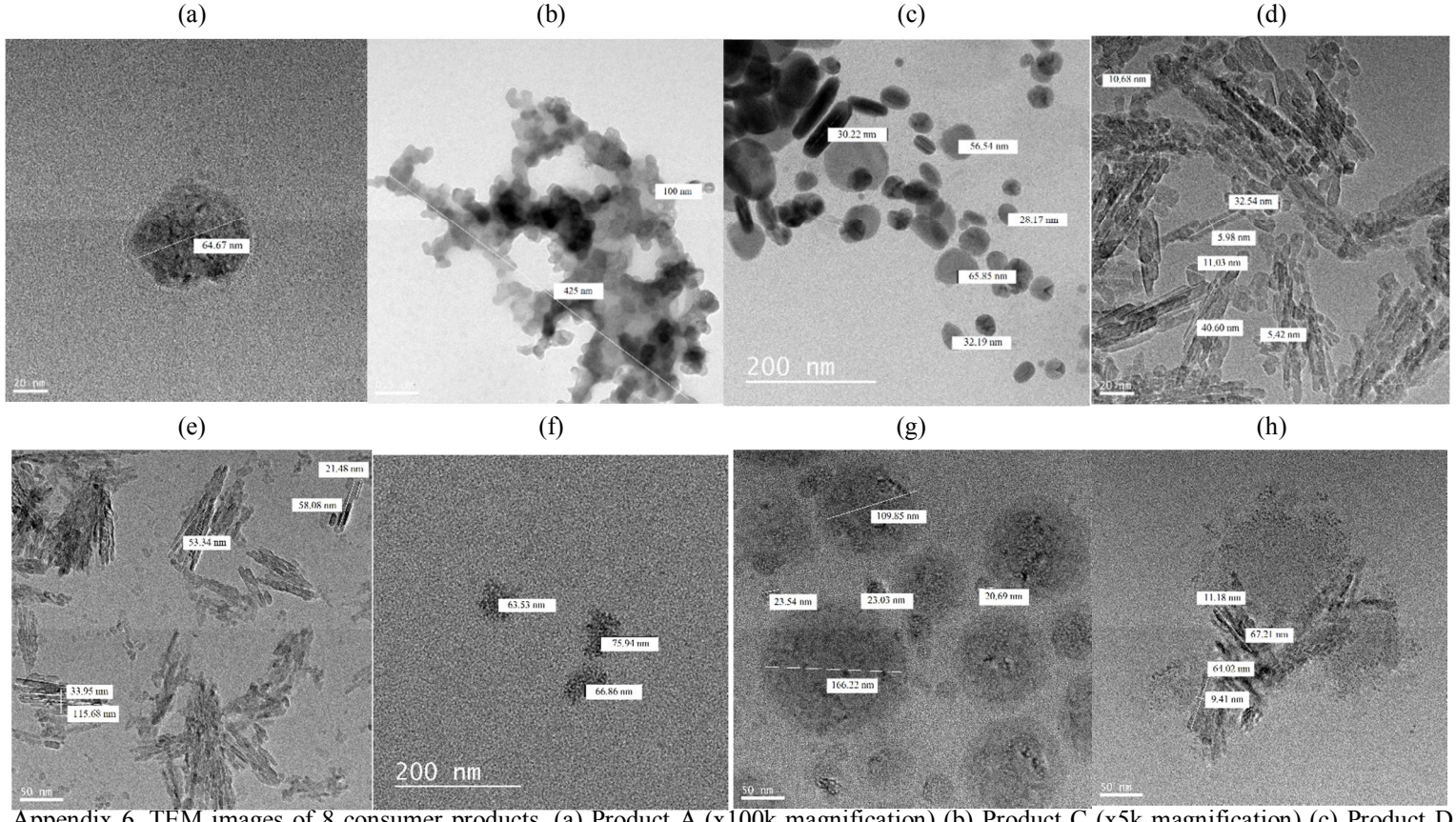

Appendix 6. TEM images of 8 consumer products. (a) Product A (x100k magnification) (b) Product C (x5k magnification) (c) Product D (x100 magnification) (d) Product F (x100k magnification) (e) Product G (x50k magnification) (f) Product H (x100 magnification) (g) Product I (x50k magnification) (h) Product J (x50k magnification).